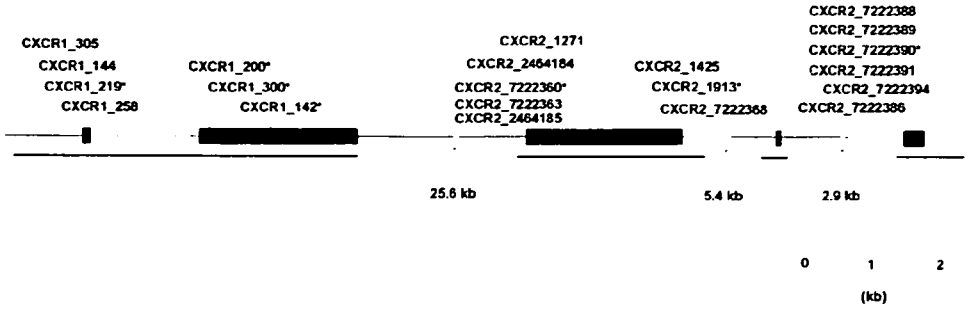

Fig. 1. Physical map of the human CXCR1 and CXCR2 genes. Coding and untranslated regions are indicated by black and gray bars, respectively. The location of polymorphisms with frequencies of >1% is indicated. The asterisk corresponds to polymorphisms that are in strong LD. A horizontal line below each gene shows the regions that have been sequenced.

alleles at these six sites constituted a single haplotype with an estimated frequency of 3.9% (*CXCR1–2_H3* in Table 2). Nearly complete LD was also observed with *CXCR2_1913*.

Reduction of Cell-Surface Expression of CD4 and CXCR4 in *CXCR1-Ha* Cells. To evaluate biological function of the two *CXCR1* nonsynonymous variants, we established transfectants of the *CXCR1-HA* and *CXCR1-Ha* haplotypes, in which HA and Ha incorporate the major and minor alleles, respectively, at both the *CXCR1_300* and the *CXCR1_142* sites (Table 2). Cell-surface expression of the HIV receptor CD4 and coreceptors CXCR4 and CCR5 was assessed on human osteosarcoma (HOS) cells after introduction of *CXCR1* variant cDNAs (see *Materials and Methods*). Flow cytometric analysis showed a reduction of cell-surface expression of CD4 and CXCR4 in *CXCR1-Ha* cells compared with *CXCR1-HA* cells (Fig. 2*A*). Western blotting and RT-PCR showed that the expression of CD4 protein and the amount of CD4 mRNA were markedly lower in *CXCR1-Ha* compared with *CXCR1-HA* cells, whereas CCR5 was unaffected (Fig. 2 *B* and *C*). Reduced expression of CXCR4 was also confirmed at a protein level by Western blotting, although no clear difference of mRNA amount was detected by RT-PCR. (Fig. 2 *B* and *C*). We then examined whether variant cDNAs also affects levels of endogenous CD4 and CXCR4 molecules by transfection experiments using Jurkat human T lymphocytes. Reduced expression of CD4 was observed in Jurkat *CXCR1-Ha* cells compared with Jurkat *CXCR1-HA* cells by flow cytometry, Western blotting and RT-PCR (Fig. 2 *D–F*). Endogenous CD4 and CXCR4 showed similar patterns in another T lymphocyte cell line, CEM cells, transfected with variant cDNAs (results not shown).

The cell-surface expression levels of *CXCR1-HA* and *CXCR1-Ha* were found to be similar (Fig. 3*A*). The intracellular [Ca^{2+}] mobilization, receptor endocytotic activity, and chemotactic activity were slightly reduced in *CXCR1-Ha* cells as compared with *CXCR1-HA* cells (Fig. 3 *B–D*). Biological consequences of these phenomena still remain to be investigated. Immunohistochemical analysis revealed that the distribution of CD4 at the plasma

Table 1. Summary of genetic polymorphisms in the human CXCR1 and CXCR2 genes

Polymorphisms						Frequencies A1			*P* values for statistical tests (when <0.01)		
Gene	CNG ID	Position	Location	A1	A2	CTR	SP	RP	CTR vs. SP vs. RP	RP vs. NP	dbSNP ID
CXCR1	305	−2668	Promoter	G	A	0.95	0.95	0.95	—	—	rs2671222
	144	−2423	Promoter	G	A	0.98	0.98	0.99	—	—	rs17838611
	219	−2329	Promoter	C	T	0.96	0.94	1.00	0.0008	0.0003	rs16858841
	258	−1566	Intron	C	G	0.94	0.95	0.95	—	—	rs3138060
	200	−143	Intron	C	T	0.96	0.94	1.00	0.0008	0.0003	rs16858816
	300	92	Exon (Met/Arg)	T	G	0.96	0.94	1.00	0.001	0.0003	rs16858811
	142	1003	Exon (Arg/Cys)	C	T	0.96	0.94	1.00	0.001	0.0002	rs16858808
CXCR2	7222388	−9203	Promoter	A	G	0.57	0.59	0.55	—	—	rs3890158
	7222389	−9191	Promoter	—	T	0.57	0.59	0.56	—	—	ss69355493
	7222390	−9185	Promoter	T	G	0.96	0.93	1.00	0.0004	0.0003	rs3890157
	7222391	−9179	Promoter	T	—	0.52	0.59	0.57	—	—	ss69355494
	7222394	−8909	Promoter	T	C	0.52	0.52	0.54	—	—	rs4674258
	7222386	−8490	Exon (5′-UTR)	A	G	0.57	0.59	0.55	—	—	rs4674259
	7222368	−270	Intron	G	A	0.53	0.54	0.54	—	—	ss69355495
	1913	768	Exon (Val/Val)	C	T	0.95	0.93	0.99	0.0015	0.0006	rs11574750
	1425	786	Exon (Leu/Leu)	C	T	0.52	0.51	0.51	—	—	rs2230054
	1271	936	Exon (Leu/Leu)	C	T	0.99	0.99	0.99	—	—	ss69355496
	2464184	1209	Exon (3′-UTR)	C	T	0.57	0.58	0.51	—	—	rs1126579
	7222360	1420	Exon (3′-UTR)	A	G	0.96	0.94	1.00	0.0004	0.0002	rs13306441
	7222363	1437	Exon (3′-UTR)	C	T	0.01	0.01	0.01	—	—	ss69355497
	2464185	1441	Exon (3′-UTR)	G	A	0.53	0.53	0.54	—	—	rs1126580

The position of each SNP was counted on the reference sequence (NT_005403.10) from the first nucleotide of the initiation codon as +1. A1 represents the nucleotide identical to that of the reference sequence. Single Nucleotide Polymorphism Database (dbSNP) IDs are also given for those that are already reported and registered on dpSNP (www.ncbi.nlm.nih.gov/SNP). *P* values for comparisons of the allele frequencies in the specified series are shown when <0.05. For these comparisons, adjustment for multiple testing (see *Methods*) gave $P < 0.01$ in all instances except for the CTR vs. SP vs. RP comparison of *SNP_7222390* in *CXCR2* ($P = 0.02$). CNG, Centre National de Génotypage.

Table 2. Haplotypes of *CXCR1* and *CXCR2* sites that are associated with disease progression

	Polymorphisms								Haplotype distribution						*P* value	
									CTR		SP		RP		CTR vs. SP vs. RP	SP vs. RP
Haplotypes	219	200	300	142	7222390	7222391	1913	7222360	Counts	Freq	Counts	Freq	Counts	Freq	Corrected	
CXCR1_HA	C	C	T	C	—	—	—	—	903/942	0.958	496/526	0.943	172/172	1.000	0.00083	0.00029
CXCR1_Ha	T	T	G	T	—	—	—	—	39/942	0.041	30/526	0.057	0/172	0.000	0.00083	0.00029
CXCR2_H1	—	—	—	—	T	—	C	A	446/940	0.474	271/524	0.516	96/170	0.565	0.053	0.290
CXCR2_H2	—	—	—	—	T	T	C	A	445/940	0.474	217/524	0.415	73/170	0.429	0.077	0.721
CXCR2_H3	—	—	—	—	G	—	T	G	39/940	0.041	31/524	0.059	0/170	0.000	0.00064	0.00018
CXCR2_H4	—	—	—	—	T	—	T	A	10/940	0.010	5/524	0.009	1/170	0.006	0.923	1.000
CXCR1-2_H1	C	C	T	C	T	—	C	A	447/938	0.474	272/522	0.517	97/172	0.564	0.054	0.334
CXCR1-2_H2	C	C	T	C	T	T	C	A	444/938	0.472	218/522	0.415	74/172	0.430	0.096	0.790
CXCR1-2_H3	T	T	G	T	G	—	T	G	37/938	0.039	29/522	0.055	0/172	0.000	0.00108	0.00029
CXCR1-2_H4	C	C	T	C	T	—	T	A	10/938	0.010	3/522	0.006	1/172	0.006	0.839	1.000

Freq, frequency.

membrane coincided with *CXCR1-HA*, but not with *CXCR1-Ha* (Fig. 3*E*).

We then examined whether the *CXCR1-Ha* haplotype correlates lower CD4 expression under physiological conditions. Of ≈2,800 healthy Thai volunteers, we chose 8 subjects heterozygous for the *CXCR1* allele (*CXCR1-HA/Ha*) and 11 wild-type homozygotes (*CXCR1-HA/HA*). Because of a low frequency (5.3%) of the *CXCR1-Ha* allele in Thai population, we couldn't include individuals homozygous for the *CXCR1-Ha* allele. Expression of the cell surface CD4 was performed by using flow cytometry by measuring the mean fluorescence intensity (MFI) of $CXCR1^+/CD4^+$ fraction of peripheral blood leukocytes. Although a tendency of lower CD4 expression levels was observed in individuals carrying *CXCR1-HA/Ha* (MFI: 224.57 ± 41.13) than in those with *CXCR1-HA/HA* (MFI: 234.82 ± 29.53), the difference was not statistically significant, probably due to a limited number of individuals examined.

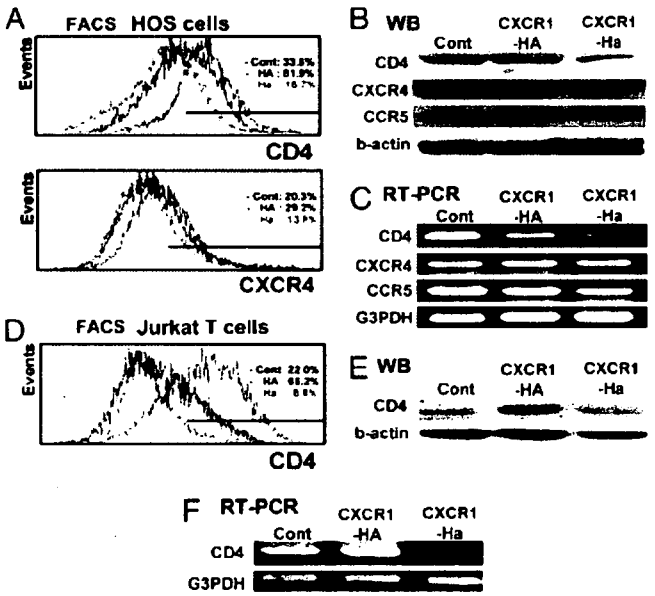

Fig. 2. Expression of HIV receptor/coreceptor on HOS cells (*A–C*) or Jurkat cells (*D–F*). (*A*) Flow cytometric analysis of HIV receptor CD4 and coreceptor CXCR4. (*B* and *C*) Western blot analysis (*B*) and RT-PCR analysis (*C*) of HIV receptor CD4, and coreceptors CXCR4 and CCR5. (*D*) Flow cytometric analysis of HIV receptor CD4. (*E* and *F*) Western blot analysis (*E*) and RT-PCR analysis (*F*) of HIV receptor CD4. A representative result from three independent experiments is shown.

Future examinations employing individuals who are homozygous for the *CXCR1-Ha* allele, a rare subset of the population, will provide a conclusive answer to this issue.

***CXCR1-Ha* Has an Inhibitory Effect on HIV Infection.** It is of interest to examine whether CXCR1 variability influences the efficiency of HIV-1 infection *in vitro*. We first analyzed the infection efficiency of X4-tropic HIV-1_{NL4-3} strain to HOS *CXCR1-HA* and *CXCR1-Ha* transfectants by using HIV p24 expression as a marker. After HIV-1_{NL4-3} exposure, *CXCR1-Ha* cells showed lower HIV p24 expression compared with control cells (transfected only with empty vector), whereas *CXCR1-HA* cells exhibited enhanced p24 levels (Fig. 4*A*). There was no significant difference in p24 levels between *CXCR1-Ha* and *CXCR1-HA* cells when R5-tropic HIV was used (data not shown). These results were further confirmed by a series of experiments with HIV-1 clinical isolates obtained from AIDS patients with or without syncytia formation in MT-2 cells (termed S.I. or N.S.I., respectively). *CXCR1-Ha* transfectants showed significantly lower p24 expression compared with *CXCR1-HA* transfectants in all of the isolates (Fig. 4), demonstrating an inhibitory effect of the Ha-variant allele on HIV-1 infection. Interestingly, p24 levels in *CXCR1-HA* cells were consistently similar to control cells in the experiments with HIV-1 isolates from patients without syncytia formation (Fig. 4*C*), whereas they were consistently increased in HIV-1 isolates from patients with syncytia (Fig. 4*B*) and X4-tropic HIV-1_{NL4-3} strain (Fig. 4*A*). This finding may reflect the content of X4-tropic HIV-1 in isolates; S.I. isolates are from patients in later stages of disease and thus richer in X4-tropic HIV-1. Increased cell-surface CXCR4 expression in *CXCR1-HA* cells may result in higher p24 levels. When using N.S.I. isolates with a lesser content of X4-tropic HIV-1, the difference of p24 expression became smaller between control cells and *CXCR1-HA* cells. The possibility of the involvement of R5-tropic HIV-1 in reduction of infection efficiency in *CXCR1-Ha* cells is also conceivable. In all instances, *CXCR1-Ha* cells had lower p24 expression than control cells.

Predominant Role of *CXCR1_142* Over *CXCR1_300*. Additional transfection experiments were undertaken with HOS cells by using artificial constructs of *CXCR1* cDNA that carry a single variation, either at *CXCR1_142* or *CXCR1_300*. These experiments allowed us to map the effect on CD4 expression on the cell surface to the *CXCR1_142* site and exclude a major effect of *CXCR1_300* (results not shown). Other data also support a predominant role for *CXCR1_142* over *CXCR1_300*. The minor allele at *CXCR1_142* introduces a cysteine residue in the C terminus intracellular domain, which is a target of palmitoylation in most chemokine receptors. Palmitoylation influences receptor trafficking and signal

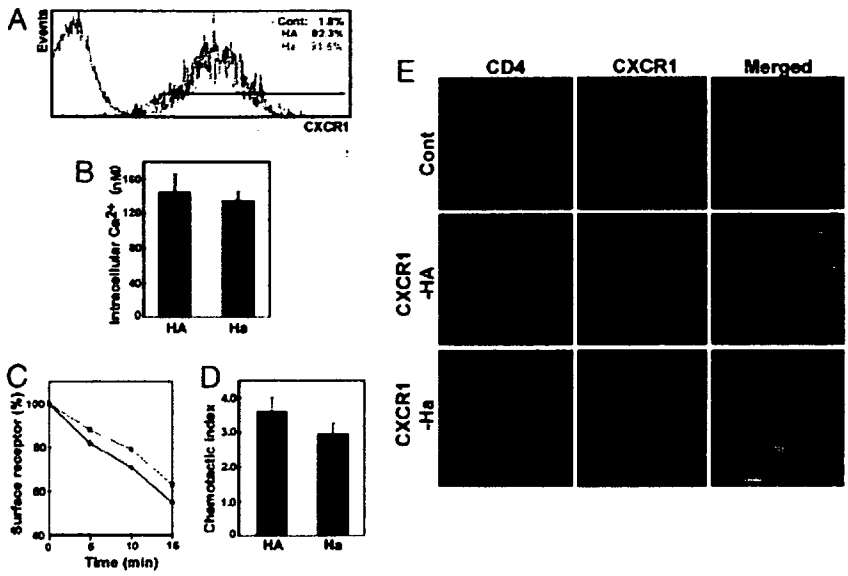

Fig. 3. CXCR1 expression and cellular responses to its cognate ligand IL-8 by using HOS cells. (*A*) Flow cytometric analysis of CXCR1 expression. (*B*) Intracellular Ca^{2+} mobilization. (*C*) Receptor internalization. (*D*) Chemotactic activity. (*E*) Confocal fluorescence microscopic images showing the subcellular distribution of CD4 (left column, green) and *CXCR1-HA* or *CXCR1-Ha* (middle column, red) on each transfected HOS cells. Overlaid green and red images show the colocalization between CD4 and CXCR1 (right column, yellow).

transduction by altering interaction with signaling and regulatory proteins (20). Moreover, extensive site-directed mutagenesis studies have failed to demonstrate significance of the methionine substitution at the *CXCR1_300* position for IL-8 binding and calcium flux (21).

Association of CXCR1 and CXCR2 SNPs with AIDS Progression. The relationship of the 21 variants of *CXCR1* and *CXCR2* to AIDS progression was evaluated by genotyping of the GRIV cohort (22), consisting of 253 asymptotic HIV-1 seropositive individuals (SP series) and 84 patients with rapid disease progression (RP series). To validate the cohort, we examined the *CCR5 delta-32* polymorphism. The results are compatible with previous studies in which *CCR5 delta-32* has been shown to restrict infection in homozygous individuals and to reduce disease progression in the heterozygous state in Caucasians (8–10, 23). We found no individuals homozygous for the *CCR5 delta-32* allele in GRIV compared with two individuals in the CTR series. The frequency of *CCR5 delta-32* was 12% in the SP series, 7% in the CTR series, and 2% in the RP series ($P = 0.0002$), confirming its association with progression.

The frequencies of the common *CXCR1–CXCR2* polymorphisms in the CTR, SP, and RP series are shown in Table 1. Significant differences in allele frequencies among the groups were found for seven SNPs ($P < 0.001$). Of particular interest, only the two sites involving nonsynonymous amino acid substitutions (*CXCR1_300* and *CXCR1_142*) and the others in strong LD with these (*CXCR1_219*, *CXCR1_200*, *CXCR2_7222390*, and *CXCR2_7222360*) showed significant frequency differences. At these six sites, the minor alleles were absent in the RP series, whereas the corresponding frequencies of these alleles in the SP and CTR series were ≈6% and ≈4%, respectively. The most extreme allele frequencies in the SP and RP series, with the CTR intermediate, is similar to those in *CCR5* and compatible with association to progression. The haplotype carrying the minor alleles at the six strongly associated sites (designated *Ha*) was absent in the RP series and has significantly higher frequencies in SP and CTRs ($P = 0.001$ for SP vs. CTR vs. RP; $P = 0.0003$ for SP vs. RP; see Table 2). To determine if these associations could be due to variants in neighboring genes in LD with a *CXCR1–CXCR2* locus, we performed SNP identification of the two flanking genes, *ARPC2* (50-kb telomeric to *CXCR1*) and *FLJ46536* (35-kb centromeric to *CXCR2*). None of the polymorphisms detected exhibited significant LD with *CXCR1* or *CXCR2* variants, demonstrating that the disease-associated haplotype does not extend to the neighboring genes.

Discussion

Our results afford strong biological and genetic evidence of a protective role of *CXCR1* variants on HIV-1 disease progression. As discussed above, the *CCR5 delta-32* variant is also known to be associated with resistance to $CD4^+$ cell depletion, but different mechanisms are likely to underlie between the involvement of CCR5 and CXCR1 in disease progression. *CCR5 delta-32* gives rise to a truncated CCR5 molecule that forms heterocomplexes with intact CCR5 in the endoplasmic reticulum, leading to reduced CCR5 cell-surface density and contributing to slower disease progression in heterozygotes (8–10). The major effect of the reduced CCR5 density appears to be modulation of virus replication cycle in early stages, particularly of reverse transcription (24).

In contrast, the inhibitory effects of variant CXCR1 on the X4-tropic HIV-1 infection are likely to be a consequence of the suppressed expression of CD4 and CXCR4. The importance of CXCR1 in disease progression may be related to the Th1-to-Th2 shift observed in the later stages of AIDS. In atopic patients, this shift has been associated with an increase of $CXCR1^+CD4^+$ cells (25). The lower expression of CD4 and CXCR4 in *CXCR1-Ha* cells demonstrated in our study could be caused by unknown CXCR1-mediated signaling that regulates expression and intracellular trafficking of CD4 and CXCR4. Coexpression of CCR5 and CXCR4 interferes with HIV-1 entry under low density of cell surface CD4 (26), and the appearance of CXCR4 tropic HIV-1 variants in later stages of infection is associated with a decline in $CD4^+$ T cell counts and adverse clinical prognosis of AIDS (25). Direct involvement of reduced CXCR1-mediated signals in HIV-1 replication is also possible (18) through palmitoylation of *CXCR1-Ha* at the cysteine introduced in the C-terminal intracellular domain. Indeed, palmitoylation of C-terminal cysteine in CCR5 is known to modify receptor trafficking and activation of intracellular signaling pathways (27). Genetic association of the *CXCR1-Ha* haplotype with chronic obstructive pulmonary disease and asthma was reported (28). It is interesting to examine functional roles of the variant CXCR1 molecule in inflammatory response.

Materials and Methods

Patients and Control Subjects. The GRIV cohort was established in 1995 in France to generate a large collection of DNAs for genetic

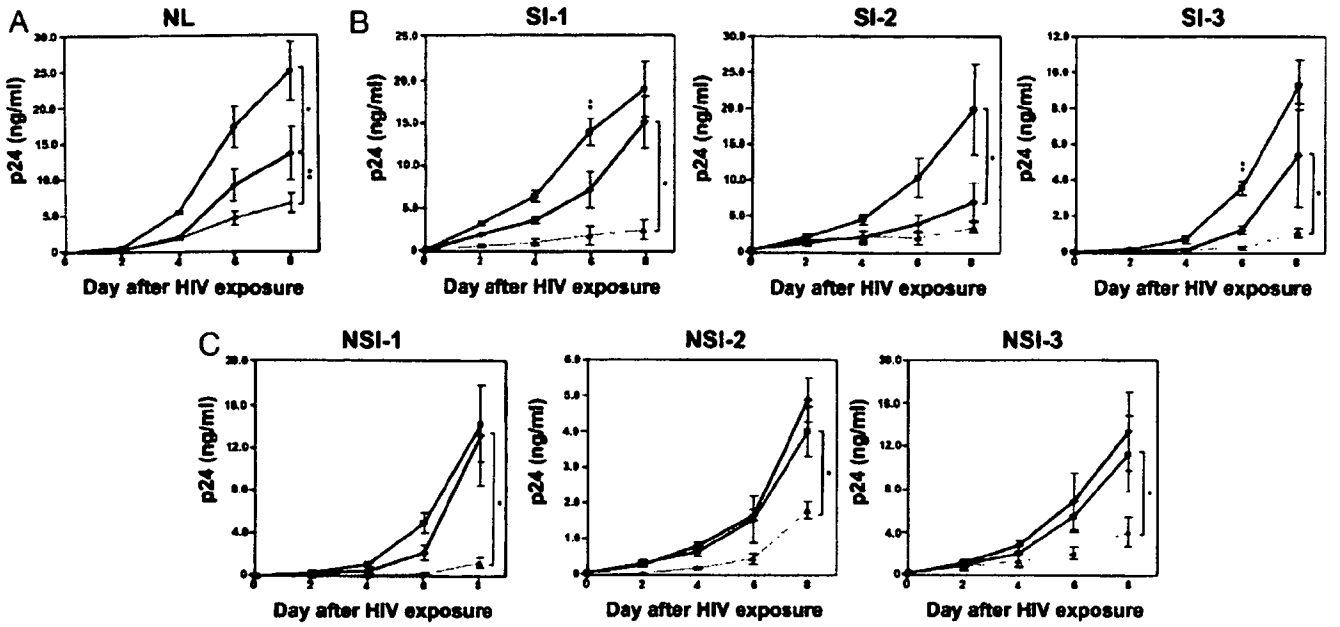

Fig. 4. The efficiency of X4-tropic HIV infection in HOS cells transfectants by using HIV-1_{NL4-3} strain (*A*), S.I. clinical isolates (*B*), and N.S.I. clinical isolates (*C*). S.I. represents an isolate with CXCR4 predominance, and N.S.I. represents and isolate with CCR5 predominance. Red, blue, and black lines show the means from three three-replicate assays for *CXCR1-Ha* (red lines), *CXCR1-HA* (blue lines) and control cells transfected with empty vector (black lines). Vertical bars indicate the range of the results obtained for each set of measurements. The amount of p24 protein in culture medium is indicated as ng/ml. Differences between *CXCR1-Ha* and *CXCR1-HA* for day 8 are significant in all instances as evaluated by a *t* test: NL, $P = 0.002$; S.I.-1, $P = 0.001$; S.I.-2, $P = 0.01$; S.I.3, $P = 0.008$; N.S.I.-1, $P = 0.003$; N.S.I.-2, $P = 0.006$; N.S.I.-3, $P = 0.03$.

studies on candidate polymorphisms associated with rapid and slow progression of AIDS (22). This cohort consists of two subpopulations with extreme phenotypes selected from a pool of ≈25,000 French HIV-1^+ individuals: 253 asymptomatic individuals with a $CD4^+$ cell count >500/mm^3 for 8 or more years after seroconversion (SP series) and 84 patients with rapid progression showing a drop in their $CD4^+$ cell count <300/mm^3 in <3 years after the last seronegative test (RP series). We estimated that the RP and SP series represented the 1% extremes of seropositive patients seen in the participating clinics in France (22). Members of the cohort were diagnosed with a seropositive test before 1996, and all are of French Caucasian origin. All patients enrolled in the study gave informed consent. The data on 471 CTR subjects of the same ethnic origin with unknown HIV status were obtained as part of the Epidemiological Study on the Genetics and Environment of Asthma (EGEA) study of asthma (29). DNA was obtained from fresh peripheral blood mononuclear cells or from EBV-transformed cell lines.

SNP Identification and Genotyping. Oligonucleotide primers were designed to amplify the exon-containing DNA fragments and the promoters by PCR [see supporting information (SI) Table 3]. Nucleotide sequencing was performed by the dye terminator method with an ABI PRISM 3700 DNA analyzer (Applied Biosystems, Foster City, CA). Results were aligned to NT_005403.10 and analyzed for SNP discovery and genotyping with the software Genalys (30). Genotypes of SNPs that showed statistical significance were reconfirmed by Taqman technology (Applied Biosystems). Information about all of the SNPs, including those with a frequency of <1%, is also available from the Centre National de Génotypage (CNG) web site (SI Table 4).

Statistics. Differences in the allele frequencies of individual polymorphisms among the three groups and between the SP and RP groups were examined by using a Fisher's exact test on the resulting 2 × 3 or 2 × 2 tables of counts. *P* values were also adjusted by performing a randomization test in which phenotype status (RP, SP, or CTR) was reassigned to the different individuals, conserving the multilocus genotypes to preserve LD. The adjusted *P* value at a specific locus was calculated as frequency over 50,000 replicates of obtaining a result at any locus as or more extreme than that observed at the specific locus. Haplotype frequencies using all polymorphisms for each gene were estimated with an EM algorithm. Differences between haplotype frequencies were examined in an analogous way to that used for the individual polymorphisms, except that within each series, expected haplotype numbers were computed from the estimated marginal haplotype probability distribution. These numbers were rounded to the nearest integer, and *P* values were computed by using Fisher's exact test.

Cell Culture, Transfection, and Flow Cytometry. HOS/CD4.CCR5 (HOS), Jurkat, and CEM cells were maintained in DMEM or RPMI medium 1640 supplement with 10% heat-inactivated FBS, 100 units/ml penicillin, and 100 mg/ml streptomycin. The coding sequences of *CXCR1* corresponding to amino acids nos. 2–350 were amplified by PCR using specific oligonucleotide primers (SI Table 3) and were inserted into the EcoRI site of the pRc/CMV-tag vector. The constructs were checked by nucleotide sequencing for the ORF, orientation and *Taq* errors. Transfections were performed by using LipofectAMINE 2000 (Invitrogen, Carlsbad, CA). Geneticin (800 μg/ml)-resistant cells were cloned by fluorescence-activated cell sorter system EPICS ELITE ESP (Beckman Coulter, Hialeah, FL). For flow cytometric analysis, transfected HOS cells were incubated with anti-CXCR1, anti-CD4, anti-CXCR4, or anti-CCR5 antibody (DAKO, Carpinteria, CA) in PBS (pH 7.3) with 0.1% FBS for 60 min at 4°C. The cells were then washed, and analyzed for cell-surface expression of the receptor by using a flow cytometry EPICS-XL (Beckman Coulter) fitted with a single 15-mW argon ion laser providing excitation at 488 nm. FITC and phycoerythrin, respectively, were monitored through 525- and 575-nm bandpass filters.

For the expression analysis of CD4 in peripheral blood leuko-

cytes, blood samples were collected in Na_2EDTA tubes and stained within 6 h. Fifty microliters of blood was gently mixed with 1 ml of red blood cell lysis buffer and incubated at room temperature for 30 min. The sample was then centrifuged at 340 × *g* for 5 min at 4°C. The leukocyte pellet was washed twice with cold PBS. The supernatant was discarded, leaving 10 μl of fluid to resuspend the cell pellet. Five microliters of anti-CXCR1 and anti-CD4 antibodies were added to the cell suspension, and the staining reaction was incubated on ice for 1 h. After centrifugation at 340 × *g* for 5 min at 4°C, the cells were washed twice with cold PBS and analyzed by a FACS machine.

RT-PCR, Western Blot Analysis, and Immunohistochemical Analysis. RT-PCR was performed according to the standard procedures with 35 cycles by using specific primers for human *CXCR1*, *CD4*, *CXCR4*, and *CCR5*. At the same time, constitutively expressed GAPDH mRNA was amplified as an internal standard. For Western blot analysis, HOS cells (5×10^5) were suspended in loading buffer [50 mM Tris (pH 7)/3% SDS/10% glycerol/5% 2-ME] and applied on polyacrylamide gel. After electrophoresis, proteins were electrotransferred to nitrocellulose membrane (Amersham Pharmacia Biotech, Piscataway, NJ), and blotted by using each primary antibody [goat anti-CD4 (C-18; Santa Cruz Biotechnology, Santa Cruz, CA), goat anti-CCR5 (CKR5; C-20; Santa Cruz Biotechnology), rabbit anti-CXCR4 (fusin; H-118; Santa Cruz Biotechnology), or mouse anti-actin antibody (C-4; Chemicon, Temecula, CA) in accordance to the manufacturer's instructions. Blots were developed with ECL reagent (Amersham Pharmacia Biotech). For immunohistochemical analysis, HOS cells were fixed with 2% paraformaldehyde in PBS, rinsed with PBS, and then treated with 0.2% Triton X-100 in PBS. The cells were incubated with fluorescence-labeled anti-CD4 and anti-CXCR1 antibodies. Images were collected with a confocal microscope (Olympus, Melville, NY).

HIV-1 Infectivity Assay. Clinical HIV-1 isolates were obtained from the plasma derived from HIV-1-infected individuals by using MAGIC-5 cells. The ability to induce syncytia formation of clinical isolates was examined in MT-2 cells. All transfected HOS cells (5×10^3) were exposed to 100 blue-cell-forming units (measured by MAGIC-5 cells) of $HIV\text{-}1_{NL4\text{-}3}$ or an HIV-1 clinical isolate in 500 μl of medium for 2 h. Infected cells were washed twice with PBS and cultured in 1 ml of medium. On days 2, 4, 6, and 8 of infection, 10-μl aliquots of culture supernatants were filtered and stocked for measurements of p24 antigen concentration. The concentration of p24 in each supernatant was determined by chemiluminescence enzyme immuno-assay (CLEIA) kit (Fuji-Rebio, Tokyo, Japan). Assays were performed in triplicate.

Intracellular $[Ca^{2+}]$ Measurement and Chemotaxis Assays. For the calcium influx study, HOS cells (10^6) were washed with Tyrode's salt solution (TSS) (Sigma, St. Louis, MO) and incubated with 4 μM Fluo-3 acetoxymethyl ester in DMSO containing 20% Pluronic F-127 (Molecular Probes, Eugene, OR) at room temperature in the dark for 1 h. After washing with the same buffer, the cells were suspended in TSS containing 0.1% BSA buffer and transferred to 96 black well plates (Nunclon) for reading. Recombinant human IL-8 (final concentration, 100 nM) was added to each sample for stimulation, and fluorescence was monitored for 3 min with the microfluorescence recorder Fluoroskan Ascent system (Labsystems, Chicago, IL). Intracellular calcium concentrations were computed as described in the manufacturer's instructions. Background stabilization and probe levels were determined for each sample. Chemotaxis of all transfected Jurkat cells in response to 10-nM recombinant IL-8 was evaluated in triplicate by using a 96-well microchemotaxis chamber (Neuro Probe, Gaithersburg, MD) and a 3-μm polycarbonate membrane. RPMI medium 1640 supplemented with 10% FBS, 0.1% BSA, and 10-mM Hepes was used for the assay. Migrated cells in the lower chamber were counted by a flow cytometer EPICS-XL (Beckman Coulter).

We thank all patients and medical staff who were concerned with the establishment of the GR1V cohort and the Epidemiological Study on the Genetics and Environment of Asthma (EGEA) cooperative group, who allowed us access to data on the EGEA study, which is partly supported by an Institut National de la Santé et de la Recherche Médicale/Merck Sharp & Dohme convention. We also thank M. Alizon for his help in the construction of the vectors for transfection experiments and M. Matsuoka for valuable suggestions. V.P., P.A., and T.S. are research members of the Core University Program, which is supported by the Japan Society for the Promotion of Science. The Centre National de Génotypage is supported by the Ministere de la Recherche et des Nouvelles Technologies. The work was supported in part by Core Research for Evolutional Science and Technology, Solution Oriented Research for Science and Technology, the Japan Science and Technology Agency, the Japan Science Foundation, Agence Nationale de Recherche sur le SIDA, and the AIDS–Cancer Vaccine Development Foundation.

1. McCune JM (2001) *Nature* 410:974–979.
2. Taylor JM, Tan SJ, Detels R, Giorgi JV (1991) *AIDS* 5:159–167.
3. Haynes BF, Pantaleo G, Fauci AS (1996) *Science* 271:324–328.
4. Cocchi F, DeVico AL, Garzino-Demo A, Arya SK, Gallo RC, Lusso P (1995) *Science* 270:1811–1815.
5. Deng H, Liu R, Ellmeier W, Choe S, Unutmaz D, Burkhart M, Di Marzio P, Marmon S, Sutton RE, Hill CM, *et al.* (1996) *Nature* 381:661–666.
6. Dragic T, Litwin V, Allaway GP, Martin SR, Huang Y, Nagashima KA, Cayanan C, Maddon PJ, Koup RA, Moore JP, Paxton WA (1996) *Nature* 381:667–673.
7. Feng Y, Broder CC, Kennedy PE, Berger EA (1996) *Science* 272:872–877.
8. Samson M, Libert F, Doranz BJ, Rucker J, Liesnard C, Farber CM, Saragosti S, Lapoumeroulie C, Cognaux J, Forceille C, *et al.* (1996) *Nature* 382:722–725.
9. Dean M, Carrington M, Winkler C, Huttley GA, Smith MW, Allikmets R, Goedert JJ, Buchbinder SP, Vittinghoff E, Gomperts E, *et al.* (1996) *Science* 273:1856–1862.
10. Liu R, Paxton WA, Choe S, Ceradini D, Martin SR, Horuk R, MacDonald ME, Stuhlmann H, Koup RA, Landau NR (1996) *Cell* 86:367–377.
11. Baggiolini M, Dewald B, Moser B (1997) *Annu Rev Immunol* 15:675–705.
12. Schroder JM, Mrowietz U, Morita E, Christophers E (1987) *J Immunol* 139:3474–3483.
13. Yoshimura T, Matsushima K, Tanaka S, Robinson EA, Appella E, Oppenheim JJ, Leonard EJ (1987) *Proc Natl Acad Sci USA* 84:9233–9237.
14. Larsen CG, Anderson AO, Appella E, Oppenheim JJ, Matsushima K (1989) *Science* 243:1464–1466.
15. Matsumoto T, Miike T, Nelson RP, Trudeau WL, Lockey RF, Yodoi J (1993) *Clin Exp Immunol* 93:149–151.
16. Meddows-Taylor S, Martin DJ, Tiemessen CT (1999) *Clin Diagn Lab Immunol* 6:345–351.
17. Meddows-Taylor S, Martin DJ, Tiemessen CT (1998) *J Infect Dis* 177:921–930.
18. Lane BR, Lore K, Bock PJ, Andersson J, Coffey MJ, Strieter RM, Markovitz DM (2001) *J Virol* 75:8195–8202.
19. Richardson RM, Tokunaga K, Marjoram R, Sata T, Snyderman R (2003) *J Biol Chem* 278:15867–15873.
20. Qanbar R, Bouvier M (2003) *Pharmacol Ther* 97:1–33.
21. Leong SR, Kabakoff RC, Hebert CA (1994) *J Biol Chem* 269:19343–19348.
22. Hendel H, Cho YY, Gauthier N, Rappaport J, Schachter F, Zagury JF (1996) *Biomed Pharmacother* 50:480–487.
23. Rappaport J, Cho YY, Hendel H, Schwartz EJ, Schachter F, Zagury JF (1997) *Lancet* 349:922–923.
24. Lin YL, Mettling C, Portales P, Reynes J, Clot J, Corbeau P (2002) *Proc Natl Acad Sci USA* 99:15590–15595.
25. Connor RI, Sheridan KE, Ceradini D, Choe S, Landau NR (1997) *J Exp Med* 185:621–628.
26. Lee S, Lapham CK, Chen H, King L, Manischewitz J, Romantseva T, Mostowski H, Stantchev TS, Broder CC, Golding H (2000) *J Virol* 74:5016–5023.
27. Blanpain C, Wittamer V, Vanderwinden JM, Boom A, Renneboog B, Lee B, Le Poul E, El Asmar L, Govaerts C, Vassart G, *et al.* (2001) *J Biol Chem* 276:23795–23804.
28. Stemmler S, Arinir U, Klein W, Rohde G, Hoffjan S, Wirkus N, Reinitz-Rademacher K, Bufe A, Schultze-Werninghaus G, Epplen JT (2006) *Genes Immun* 6:225–230.
29. Kauffmann F, Dizier MH, Pin I, Paty E, Gormand F, Vervloet D, Bousquet J, Neukirch F, Annesi I, Oryszczyn MP, *et al.* (1997) *Am J Respir Crit Care Med* 156:S123–S129.
30. Takahashi M, Matsuda F, Margetic N, Lathrop M (2003) *J Bioinform Comput Biol* 1:253–265.

Altering Effects of Antigenic Variations in HIV-1 on Antiviral Effectiveness of HIV-Specific CTLs[1]

Takamasa Ueno,[2]* Yuka Idegami,* Chihiro Motozono,* Shinichi Oka,†‡ and Masafumi Takiguchi*

The mutational escape of HIV-1 from established CTL responses is becoming evident. However, it is not yet clear whether antigenic variations of HIV-1 may have an additional effect on the differential antiviral effectiveness of HIV-specific CTLs. Herein, we characterized HIV-specific CTL responses toward Pol, Env, and Nef optimal epitopes presented by HLA-B*35 during a chronic phase of HIV-1 infection. We found CTL escape variants within Pol and Nef epitopes that affected recognition by TCRs, although there was no mutation within the Env epitope. An analysis of peptide-HLA tetrameric complexes revealed that CD8 T cells exclusively specific for the Nef variant were generated following domination by the variant viruses. The variant-specific cells were capable of killing target cells and producing antiviral cytokines but showed impaired Ag-specific proliferation ex vivo, whereas wild-type specific cells had potent activities. Moreover, clonotypic CD8 T cells specific for the Pol variant showed diminished proliferation, whereas Env-specific ones had no functional heterogeneity. Taken together, our data indicate that antigenic variations that abolished TCR recognition not only resulted in escape from established CTL responses but also eventually generated another subset of variant-specific CTLs having decreased antiviral activity, causing an additional negative effect on antiviral immune responses during a chronic HIV infection. ***The Journal of Immunology,*** **2007, 178: 5513–5523.**

Virus-specific $CD8^+$ CTLs play a critical role in the control of persistent virus infections including those by HIV-1. However, recent studies show that HIV-specific CD8 T cell responses, measured by their ability to bind with peptide-HLA class I tetrameric complexes (HLA tetramers) or to secrete IFN-γ Ag specifically, are not correlated with the control of viremia in chronic HIV-1 infections (1, 2), suggesting a progressive functional defect in HIV-specific CTLs during a chronic infection that is not measurable by these assays. Accordingly, HIV-specific CD8 T cells in individuals with a primary infection and individuals with a long-term nonprogressive infection exhibit strong Ag-dependent ex vivo proliferative capacity, whereas those from patients with a progressive disease course lose such capacity (3–5). In addition, recent reports show that various degrees of impairment of the effector functions of virus-specific CD8 T cells are influenced by Ag persistence and Ag levels in mice and humans (5–8), suggesting that antiviral effectiveness of HIV-specific CD8 T cells can be impaired through repeated stimulation by the same cognate Ags. In contrast, it is reported that significant differences also exist in the effectiveness of HIV-specific CTLs among different specificities and restricting elements (9, 10), as well as among TCR clonotypes within the same specificity (11, 12). Therefore, different Ags or a set of amino acid substitutions within an Ag may be involved differently in the generation of the altered antiviral effectiveness of HIV-specific CTLs.

It is becoming evident that the mutational escape of HIV from established CTL responses occurs in individual human hosts (13, 14). CTL escape mutations occur at critical sites in the CTL epitopes in the viral genome or in the flanking sequences encoding these epitopes, leading to altered Ag processing (15, 16), loss of peptide-HLA binding, or loss of TCR recognition. The two former consequences of these mutations result in the ultimate loss of epitopes to be presented on the surface of virus-infected cells for recognition by CTLs. In contrast, the latter consequence is thought to provide a relatively weak selective advantage for HIV, because this type of mutation results in the loss of recognition by some existing CTL lines while maintaining recognition by other cross-recognizing CTL subsets. It is not clear why mutations that affect TCR recognition are selected in the virus under CTL-mediated immune pressure even though they can provide only moderate selective advantage for the virus.

In the present study, we focused on CD8 T cell responses specific for the HIV-1 Pol, Env, and Nef optimal epitopes presented by HLA-B*35 in patients at the chronic phase of HIV-1 infection to ask whether and how antigenic variations of HIV-1 have an additional effect on the altered antiviral activity of HIV-specific CTLs. Sequence analysis of autologous viruses showed the existence of HLA-B*35-associated mutations within Pol and Nef epitopes that affected TCR recognition. HLA tetramer analysis revealed that the Nef variant-specific CD8 T cells were generated following domination by the variant viruses. The variant-specific cells had the ability to kill target cells and secrete antiviral cytokines but, interestingly, they showed impaired proliferation activity ex vivo. Similar defects in proliferative capacity were also observed in the variant Pol-specific CD8 T cells.

*Division of Viral Immunology and †Infectious Diseases, Center for AIDS Research, Kumamoto University, Kumamoto, Japan; and ‡AIDS Clinical Center, International Medical Center of Japan, Tokyo, Japan

Received for publication September 29, 2006. Accepted for publication February 9, 2007.

The costs of publication of this article were defrayed in part by the payment of page charges. This article must therefore be hereby marked *advertisement* in accordance with 18 U.S.C. Section 1734 solely to indicate this fact.

[1] This research was supported by grants-in-aid for scientific research from the Ministry of Education, Science, Sports and Culture of Japan.

[2] Address correspondence and reprint requests to Dr. Takamasa Ueno, Division of Viral Immunology, Center for AIDS Research, Kumamoto University, 2-2-1 Honjo, Kumamoto, Japan. E-mail address: uenotaka@kumamoto-u.ac.jp

Materials and Methods

Subjects

A total of seven individuals (HLA-B*35$^+$) with chronic HIV infection (>2 years) followed at the AIDS Clinical Center, International Medical Center of Japan (Tokyo, Japan) were enrolled for functional analysis of HIV-specific CD8 T cells in this study. All subjects except patient (Pt)[3] 42 (Pt-42) had been receiving antiretroviral therapy (see Table I for details). For autologous HIV-1 sequence analysis, a total of 42 individuals with chronic HIV infection (>2 years) followed at the same hospital as above were enrolled. Among them, 12 individuals expressed HLA-B*35 and the other 30 individuals did not express it. Thirty-eight of the total (11 for HLA-B*35$^+$ and 27 for HLA-B*35$^-$) had been receiving antiretroviral therapy. The study was conducted in accordance with the human experimentation guidelines of the International Medical Center of Japan and Kumamoto University (Kumamoto, Japan).

Sequence analysis of autologous HIV-1 and TCR-encoding genes

HIV-1 particles were precipitated by ultracentrifugation (50,000 rpm for 30 min) of patients' plasma, after which the viral RNA was extracted from them. A nested PCR was conducted by using sets of primers specific for the *pol*, *env*, and *nef* genes of HIV-1, as described earlier (17). PCR-amplified DNA fragments were gel purified and sequenced directly or cloned into a plasmid and then sequenced.

TCR-encoding genes of HIV-specific CD8 T cells were cloned and sequenced as previously described (18). Briefly, total RNA was prepared from T cell clones or FACS-sorted tetramer$^+$ CD8$^+$ cells, and cDNA encoding α and β TCRs were obtained by using a SMART PCR cDNA synthesis kit (Clontech Laboratories). Alignment of the V and J regions of α and β TCR genes was performed by using the ImMunoGeneTics database (http://imgt.cines.fr) created by M.-P. Lefranc (Institut de Génétique Humaine, Montpellier, France) (19).

Construction of Nef-expressing target cells

For target cells endogenously expressing Nef-GFP fusion proteins, DNA fragments encoding the Nef protein (HIV-1 NL43) and GFP were cloned into plasmid pcDNA3.1 (Invitrogen Life Technologies). A mutation, Met^{20} to Ala, was introduced to abolish HLA class I down-regulation activity by Nef (20), and the Thr^{75} to Arg mutation was achieved by site-directed mutagenesis. The m^{7}GpppG-capped and poly(A)-tailed mRNAs were prepared in vitro by using a mMessage mMachine T7 Ultra kit (Ambion).

The mRNA samples were delivered to target cells by electroporation. Briefly, cells were suspended in a serum-free medium (Opti-MEM; Invitrogen Life Technologies) at the cell density of 4×10^6 cells/ml, mixed with 10 μg of mRNA, and electroporated by using a Gene Pulser device (Bio-Rad). The cells were immediately transferred to medium (RPMI 1640 and 10% FBS), incubated at 37°C for 16 h, and then used as target cells. It should be noted that 15 ± 5% of the cells had died (positive for 7-aminoactinomycin D (7-AAD) staining) by 16 h and that 85 ± 5% cells of the viable cells expressed GFP as revealed by flow cytometric analysis.

Generation of T cell clones

CTL clones or lines were established by the stimulation of PBMCs with a synthetic peptide as previously described (18). Briefly, a bulk CTL culture was seeded at a density of 0.8 or 5 cells/well with a cloning mixture (irradiated allogeneic PBMC and C1R-B*3501 cells pulsed with 1 μM peptide in RPMI 1640 with 10% FCS and 100 U/ml rIL-2). Two weeks later, cells positive for growth were tested for cytolytic activity by the ^{51}Cr-release assay described below.

HLA stabilization assay

Peptide-binding activity for HLA-B*3501 was assessed by an HLA stabilization assay. RMA-S cells expressing HLA-B*3501 were cultured for 16 h at 26°C and then pulsed with various concentrations of peptide for 3 h at 26°C. The cells were then incubated at 37°C for 3 h and subsequently stained with an anti-HLA class I mAb (TP25.99). The surface expression level of HLA-B*3501 was evaluated by flow cytometry.

HLA tetramer analysis

The HLA-B*3501-tetramers in complex with a series of wild-type and variant peptides were prepared as previously described (18). Cryopreserved PBMCs of HIV-positive (2×10^6) or -negative donors (3×10^6) were stained with the tetramer at 37°C for 15 min followed by anti-CD8-PerCP (BD Biosciences) or anti-TCR Abs at 4°C for 15 min. The anti-Vδ1 mAb A13 was kindly provided by L. Moretta (University of Genova, Genova, Italy) and the other anti-TCR mAbs were purchased from Pierce Endogen and Beckman Coulter. They were then washed twice and analyzed by flow cytometry. Dead cells were gated out by 7-AAD staining as needed.

Cytotoxic assay

The cytotoxic activity of the CTL clones was determined by a standard ^{51}Cr-release assay as described previously (18). For peptide-pulsed target cells, ^{51}Cr-labeled C1R-B*3501 cells (2×10^3 cells/well) were pulsed with various concentrations of the peptide and incubated with T cells for 4 h at 37°C. For virus-infected target cells, autologous EBV-transformed B cell lines were infected with vesicular stomatitis virus envelope glycoprotein-pseudotyped HIV-1 HXB2D. It should be noted that ~75% of the cells were positive for the intracellular p24 Gag Ag when HIV-infected cells were used for CTL assays. The cells were incubated with T cells for 6 h at 37°C after having been labeled with ^{51}Cr.

For cytotoxic assays ex vivo, cryopreserved PBMCs that had been pre-incubated for 2 h at 37 °C in RPMI 1640 containing 20% FCS were separated in CD8$^+$ and CD8$^-$ subsets by using anti-CD8 mAb-conjugated magnetic beads (Miltenyi Biotec), and the resultant CD8$^+$ and CD8$^-$ cells were used for effector and target cells, respectively. Autologous EBV-transformed B cells were also used for target cells as needed. The effector cells were incubated at various ET ratios in RPMI 1640 supplemented with 10% FCS and 100 U/ml rIL-2 for 6 h and then mixed with the ^{51}Cr-labeled target cells (3000 cells/well) that had been pulsed with the wild-type and variant peptides. Cells were incubated for additional 12 h at 37°C.

Intracellular cytokine staining assay

Cryopreserved PBMC (2×10^6) of HIV-positive or -negative individuals were first incubated overnight in RPMI 1640 supplemented with 10% FCS and 200 U of IL-2. They were then incubated in the absence or presence of 1 μM Nef75 peptide (RPQVPLRPMTY or TPQVPLRPMTY) for 2 h at 37°C. Brefeldin A (10 μg/ml) was then added and the cells were incubated for an additional 4 h. Cells were permeabilized and stained with mAbs specific for IFN-γ, TNF-α, and IL-2 (BD Biosciences) as previously described (21).

Ex vivo proliferation assay

To analyze Ag-specific expansion of HLA-tetramer$^+$ cells, cryopreserved PBMCs (2×10^6) of the HIV-positive or -negative donors were first incubated as described above. They were then stimulated with irradiated EBV-transformed B cells expressing HLA-B*3501 that had been pulsed with 1 μM Nef75 peptide (RPQVPLRPMTY or TPQVPLRPMTY) or transfected with mRNA encoding GFP alone, Nef-GFP, or Nef variant-GFP fusion proteins. The cells were cultured at 37°C for 12 days in the same medium. A portion of the stimulated cells (5×10^5) were stained with HLA tetramers and anti-CD8 and anti-CD3 mAbs as previously described (12).

To further analyze proliferating cells in response to Ag stimulation, cryopreserved PBMC samples of HIV-positive donors were first incubated in RPMI 1640 containing 20% FCS for 2 h and then labeled with CFSE (Molecular Probes) as directed by the manufacturer's recommendation. Aliquots of cells (2×10^6 each) were separately incubated in RPMI 1640 with 10% FCS and 100 U/ml rIL-2 and stimulated with IL-2 alone or in combination with a cognate peptide at 1 μM concentration. After 6 days, the resultant cells were collected, stained with PE-conjugated HLA tetramers followed by anti-CD8 and anti-CD3 mAbs, and analyzed by flow cytometry. The CD3$^+$CD8$^+$ subsets were gated and the fluorescence intensity of CFSE within the tetramer$^+$ cells were analyzed.

Statistical analysis

Results were given as the mean ± SD. Statistical analysis of significance (p values) was based on paired or unpaired two-tailed t tests.

Results

*HLA-B*35-restricted CD8 T cell responses to HIV-1*

We first examined cross-sectionally the CD8 T cell responses of chronic HIV-infected patients toward HIV-1 optimal epitopes (refer to the database: http://www.hiv.lanl.gov) restricted by HLA-B*35. PBMCs isolated from HLA-B*35$^+$ patients (n = 7; see Table I for the clinical state of the subjects) were analyzed with

[3] Abbreviations used in this paper: Pt, patient; 7-AAD, 7-aminoactinomycin D; PD-1, programmed death 1.

Table I. *Longitudinal analysis of autologous virus sequence in regions within or flanking HLA-B35-restricted CTL epitopes in patients with chronic HIV infection*

Patient Identification	HLA Type	Date	CD4 (mm^{-3})	Viral Load[a]	Antiviral Therapy[b]	Pol448[c]		Env 77[c]		Nef75[c]	
						EVIPLTEEAELEL	Frequency	PTDPNPQEVVLEN	Frequency	PVRPQVPLRPMTYKGAL	Frequency
Pt-01	A2402/A2603, B3501/B4002	Oct 1995	47	ND	AZT, ddI	EVIPLTEEAELEL	Direct	PTDPNPQEVVLVN	Direct	PVTPQVPLRPMTYKAAV	Direct
		Apr 1997	146	4.5	AZT, ddC, IDV	EVVPLTEEAELEL	Direct	PTDPNPQEVVLVN	Direct	PVTPQVPLRPMTYKAAV	Direct
		Sep 1999	223	3.9	D4T, 3TC, RTV, SQV	EVVPLTEEAELEL	Direct	PTDPNPQEVVLVN	6/12	PVTPQVPLRPMTYKAAV	Direct
								PTDPNPQEVELTN	6/12		
Pt-03	A2402/A2601, B3501/B5101	May 1989	480	ND	IFN-α	EVIPLTEEAELEL	12/18	PTDPNPQEVVLVN	14/14	PVRPQVPLRPMTFKGAV	5/15
						EVVPLTEEAELEL	6/18			PVTPQVPLRPMTYKAAV	10/15
		Mar 1993	289	ND	AZT	EVIPLTEEAELEL	1/14	PTDPNPQEVVLVN	Direct	PVRPQVPLRPMTFKGAV	1/15
						EVVPLTEEAELEL	13/14			PVTPQVPLRPMTYKAAV	14/15
		May 1995	252	ND	AZT, ddI	EVVPLTEEAELEL	11/11	PTDPNPQEVVLVN	Direct	PVTPQVPLRPMTYKAAV	12/12
		Jul 1997	320	4.2	AZT, ddI, SQV	EVVPLTEEAELEL	12/12	PTDPNPQEVVLVN	Direct	PVTPQVPLRPMTYKAAV	Direct
		Jun 2002	203	3.1	ABC, TDF, LPV	EVVPLTEEAELEL	14/14	PTDPNPQEVVLVN	12/12	PVTPQVPLRPMTYKAAV	Direct
Pt-15	A11/A24, B35/B54	Jul 1996	193	3.3	3TC, d4T, NFV	EVVPLTAEAELEL	12/12	PTDPNPQEVVLVN	Direct	PVRPQVPLRPMTRRAAI	12/12
		Dec 1998	162	4.6	3TC, d4T, NFV	EVVPLTAEAELEL	Direct	PTDPNPQEVVLVN	Direct	PVTPQVPLRPMTYKAAV	12/12
		Jun 2001	383	BL	ABC, EFV, LPV	EVVPLTAEAELEL	Direct	PTDPNPQEVVLVN	Direct	PVTPQVPLRPMTYKAAV	Direct
Pt-19	A2402, B3501/B5201	Jun 1996	524	4.7	ND	EVIPLTEEAELEL	7/12	PTDPNPQEVVLVN	Direct	PVRPQVPLRPMTYKGAF	3/13
						EVVPLTEEAELEL	5/12			PVRPQVPLRPMTFKGAF	10/13
		Jul 1997	714	4.3	ND	EVVPLTEEAELEL	14/14	PTDPNPQEVVLVN	Direct	PVRPQVPLRPMTYKAAV	1/16
										PVRPQVPLRPMTFKGAF	5/16
										PVTPQVPLRPMTYKAAV	10/16
		Dec 1999	601	2.8	3TC, d4T, IDV	EVVPLTEEAELEL	Direct	PTDPNPQEVVLVN	Direct	PVTPQVPLRPMTYKAAV	14/14
		May 2001	1574	BL	d4T, 3TC, IDV	EVVPLTEEAELEL	Direct	PTDPNPQEVVLVN	Direct	PVTPQVPLRPMTYKAAV	Direct
Pt-34	A2402/A2601, B3501/B4801	May 1999	393	3.7	d4T, 3TC	EVIPLTEEAELEL	Direct	PTDPNPQEVVLVN	Direct	PVRPQVPLRPMTFKGAV	4/12
										PVTPQVPLRPMTYKAAV	8/12
		Apr 2001	201	4.4	ND	EVVPLTAEAELEL	Direct	PTDPNPQEVVLVN	Direct	PVTPQVPLRPMTYKAAV	Direct
Pt-42	A24/A31, B35/B60	Apr 1999	400	3.5	ND	EVVPLTAEAELEL	Direct	PTDPNPQEVVLVN	Direct	PVRPQVPLRPMTFKGAV	2/10
										PVTPQVPLRPMTYKAAV	8/10
		Aug 2001	311	3.8	ND	EVVPLTAEAELEL	Direct	PTDPNPQEVVLVN	Direct	PVTPQVPLRPMTYKAAV	Direct
Pt-46	A2, B35/B61	May 1999	231	BL	AZT, 3TC, IDV	EVVPLTEEAELEL	Direct	PTDPNPQEVVLVN	Direct	PVTPQVPLRPMTYKAAV	Direct
		Apr 2001	263	BL	d4T, 3TC, IDV, RTV	EVVPLTEEAELEL	Direct	PTDPNPQEVVLVN	Direct	PVTPQVPLRPMTYKAAV	Direct

[a] Viral load is log 10 copies/ml. BL, Below detection level; ND, not done.

[b] ABC, Abacavir; AZT, azidothymidine; ddI, dideoxyinosine; ddC, dideoxycytidine; d4T, didehydrothymidine; EFV, efavirenz; IDV, indinavir; LPV, lopinavir; RTV, ritonavir; SQV, saquinavir; 3TC, dideoxythiacytidine; TDF, tenofovir.

[c] Boldface letters in sequences are mutations. Epitope regions are underlined. Numbers in "Frequency" column indicate a clonal frequency of plasmid clones sequenced following the cloning of PCR-amplified DNA fragments into plasmid vectors. "Direct" indicates that the data were obtained by direct sequencing of PCR-amplified DNA fragments.

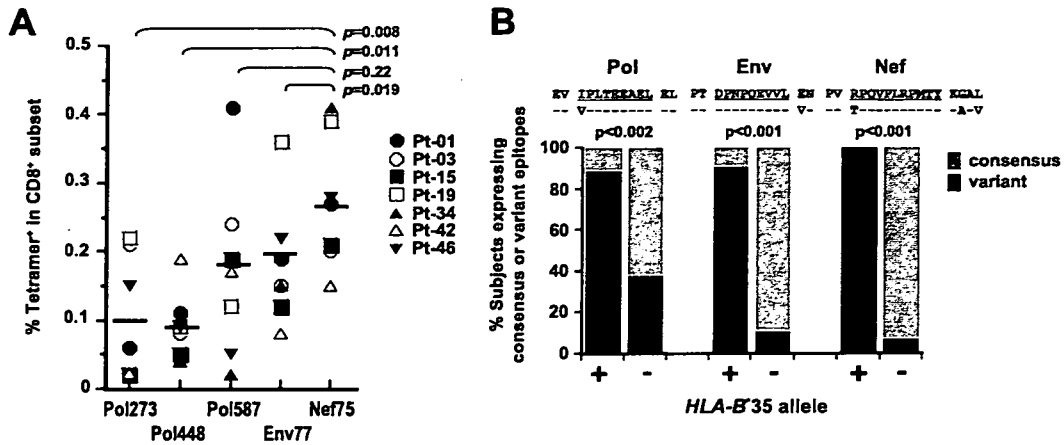

FIGURE 1. HLA-B*35-restricted CD8 T cell responses to HIV-1 and HIV-1 variants associated with *HLA-B**35 at the population level. *A*, Cryopreserved PBMC of seven HIV-infected patients were stained with HLA-B*35 tetramers in complex with the indicated peptides. The PBMC samples used for each patient were taken at the following times: Pt-01, September 1999; Pt-03, June 2002; Pt-15, June 2001; Pt-19, May 2001; Pt-34, April 2001; Pt-42, August 2001; and Pt-46, April 2001 (see Table I). The frequency of tetramer$^+$ CD8$^+$ in the total CD8$^+$ subset was plotted in the graph. Bars indicate the mean for each group. It should be noted that the background level of staining was 0.025% for all tetramers used as determined by the data from at least five HIV-negative donors (mean + 3 SD). *B*, Autologous viral RNA was prepared from chronic HIV-infected patients positive (n = 12) or negative (n = 30) for HLA-B*35. The Pol-, Env-, and Nef-encoding regions within and flanking the HLA-B*35-restricted CTL epitopes were specifically amplified by PCR and directly sequenced. Amino acid sequences indicated are clade B consensus (*upper line*) and variants associated with HLA-B*35 (*lower line*). Epitope regions are underlined and dashes denote amino acids identical with those of the clade B consensus sequence.

HLA-B35 tetramers in complex with a series of epitope peptides having clade B consensus sequences. The frequencies of tetramer$^+$ CD8$^+$ cells among the total CD8$^+$ cells were shown in Fig. 1*A* and as follows: Pol273 (VPLDKDFRKY), 0.10 ± 0.013%; Pol448 (IPLTEEAEL), 0.093 ± 0.007%; Pol587 (EPIVGAETF), 0.17 ± 0.019%; Env77 (DPNPQEVVL), 0.18 ± 0.013%; and Nef75 (RPQVPLRPMTY), 0.26 ± 0.09%. The immunodominant Nef75 epitope, subdominant Pol448 epitope, and intermediate Env77 epitope were selected for further analysis in this study.

*Evolution of HIV-1 variants associated with the HLA-B*35 allele*

The analysis of long-standing changes in autologous virus sequences of the HLA-B*35$^+$ chronic HIV-infected patients (n = 7) showed Ile to Val and Arg to Thr changes at Pol-448 and Nef-75, respectively, and Gly to Ala and Leu to Val changes in the flanking region of the Nef epitope (Table I). Despite the absence of a sequential change within the Env77 epitope, there was a substantial difference at Env86 (Table I).

Further cross-sectional analysis of the autologous virus sequence by using 42 chronic patients (12 HLA-B*35$^+$ and 30 HLA-B*35$^-$) clearly showed that the amino acid changes observed in Table I were all significantly associated with *HLA-B**35 (Fig. 1*B*), suggesting that these sequence variations were selected by CD8 T cell-mediated immune responses restricted by HLA-B*35.

Interestingly, replication-competent HIV-1 NL43 carries amino acid residues identical with those of *HLA-B**35-associated mutations, suggesting the minimal effects of these variants on the virus replication. It is also noteworthy that we found mutations in autologous viruses of HLA-B*35$^+$ patients even though most of them (11 of 12) had been receiving antiretroviral therapy, confirming a previous report showing the evolution of CTL escape mutations even when virus replication was suppressed by antiretroviral therapy (22).

Thr^{75} of Nef as a CTL escape mutation that abolished TCR recognition

By conducting an HLA stabilization assay, we first examined whether the variant peptide (Thr^{75} peptide: TPQVPLRPMTY) had lost its ability to bind with HLA-B*3501. Interestingly, the binding activity between HLA-B*3501 and the variant Thr^{75} peptide was ~10-fold higher than that of the wild-type peptide (Arg^{75} peptide: RPQVPLRPMTY), as the concentrations of the Arg^{75} and Thr^{75}

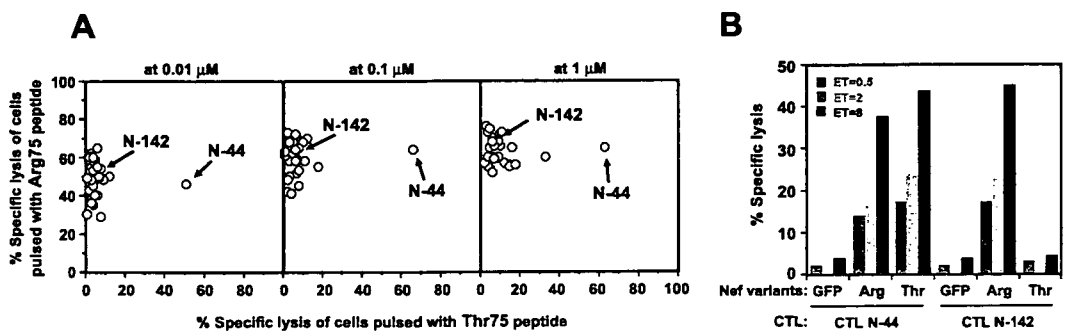

FIGURE 2. Generation of CTL clones specific for Nef and its variant in vitro. *A*, Cytotoxic activity of a representative set of 50 CTL clones toward C1R-B*3501 cells pulsed with the indicated concentrations (0.01, 0.1, and 1 μM) of the Arg^{75} or Thr^{75} peptide at an E:T ratio of 2:1. The data obtained for CTL N-44 and N-142 are indicated. Specific lysis in the absence of peptide was <5%. *B*, Cytotoxic activity of CTL clones CTL N-44 and N-142 toward C1R-B*3501 cells expressing the Arg^{75}-Nef-GFP protein, the Thr^{75}-Nef-GFP protein, or GFP alone. Of the target cells, 85 ± 5% were GFP$^+$.

Table II. *Summary of representative TCRs specific for HIV-1 antigens presented by HLA-B*35*

Specificity	Clonotypic mAb	CTL Clone	TCR Usage		
			V Region	J Region	CDR 3
Pol448	Vδ 1	CTL 55	TRDV1*01	TRAJ54*01	CALGEGGAQKLVF
			TRBV6-1*01	TRBJ2-7*01	CASRTGGTLIEQYF
	Vα 12	CTL 589	TRAV19*01	TRAJ53*01	CALSHNSGGSNYKLTFGKG
			TRBV5-4*01	TRBJ2-5*01	CASSFRGGKTQYFGPG
Env77	None	CTL E-113	TRAV26-1*01	TRAJ40*01	CIVRERGTYKYIF
			TRBV15*02	TRBJ1-1*01	CATRGGGLNTEAFF
	Vβ 5(c)	CTL E-118	TRAV13-2*01	TRAJ13*01	CAETPNSGGYQKVTF
			TRBV5-1*01	TRBJ2-1*01	CASSLFPGLAGLSSYNEQFF
Nef75	Vβ 9	CTL N-27	TRAV12-3*01	TRAJ49*01	CAMSEGTGNQFYF
			TRBV3-1*01	TRBJ2-3*01	CASSQTMGLDLTDTQYF
	Vβ 7	CTL N-44	TRAV21*02	TRAJ21*01	CAVRGTSYGKLTF
			TRBV4-1*01	TRBJ2-1*01	CASSQGPWTGVDNEQFF
	Vβ 3	CTL N-117	TRAV21*02	TRAJ24*01	CAVLKSDSWGKLQF
			TRBV28*01	TRBJ2-2*01	CASSSSTGLETTGELFF
	Vβ 3	CTL N-142	TRAV1-1*01	TRAJ3*01	CAVRGKYSSASKIIF
			TRBV28*01	TRBJ2-5*01	CASSKNRERETQYF

peptides that yielded 50% of the maximum binding level were 56.2 ± 4.6 and 5.70 ± 0.27 μM, respectively.

We then sought to generate CTL clones specific for the Arg^{75} or Thr^{75} peptide in vitro. By a 1 μM Arg^{75} peptide stimulation of PBMC (Pt-01, Pt-03, and Pt-19), >50 CTL clones were generated. The cytotoxic activity of these CTL clones toward cells pulsed with the Arg^{75} or Thr^{75} peptide showed that all clones except one were exclusively specific for the Arg^{75} peptide (Fig. 2*A*). The $V\beta3^+$ T cells showed ~50% frequency among the Arg^{75}-specific CTL clones, and TCR usage of representative Arg^{75}-specific CTL clones (CTL N-27, N-117, and N-142) is shown in Table II. Remarkably, only one of >50 CTL clones (CTL N-44; Fig. 2*A*), which had $V\beta7^+$ TCR (Table II), showed cytotoxic activity toward cells pulsed with either Arg^{75} or Thr^{75} peptides, although an additional CTL clone showed partially cross-reactive capacity at the high concentrations of the Thr^{75} peptide (Fig. 2*A*). These data suggested an extremely low frequency of precursors of such cross-reactive CD8 T cells in these subjects (see below).

Next, we found that the cross-reactive CTL N-44 had comparable killing activity toward C1R-B*3501 cells expressing either the Arg^{75}- or Thr^{75}-Nef-GFP fusion protein (Fig. 2*B*), indicating that the Thr^{75} peptide was endogenously processed and extracellularly presented by HLA-B*3501 for CTL recognition. Moreover, a representative Arg^{75}-specific CTL clone, CTL N-142, showed killing activity toward cells expressing the Arg^{75}-GFP fusion protein but not toward those expressing the Thr^{75}-GFP one (Fig. 2*B*), indicating again that Thr^{75} was a CTL escape mutation that abolished TCR recognition.

It should be noted, however, that despite a number of attempts we failed to generate Thr^{75}-specific CTL clones or lines by stimulating the PBMCs of all seven patients with the Thr^{75} peptide although the samples were taken when their autologous HIV-1 had

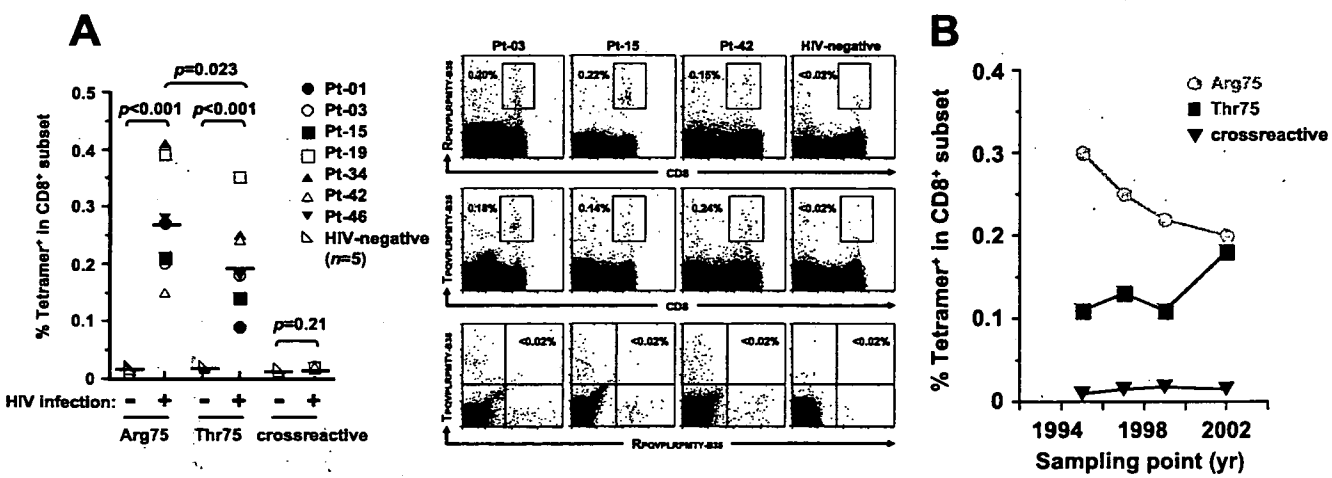

FIGURE 3. CD8 T cell responses toward Nef and its variant ex vivo. *A*, PBMCs of seven HIV-infected patients, the same as those used in Fig. 1*A*, and five HIV-negative donors were stained with PE and allophycocyanin-conjugated HLA-B*35 tetramers in complex with the Arg^{75} and Thr^{75} peptides, respectively. After the dead cells had been gated out by staining with 7-AAD, the remaining cells were analyzed for their binding to each of the tetramers and for their cross-reactivity. The frequency of $tetramer^+CD8^+$ in the total $CD8^+$ subset was plotted in the graph. Bars indicate the mean for each group. Representative dot plots for three HIV-infected subjects (Pt-03, Pt-15, and Pt-42) and a HIV-negative donor are shown with $tetramer^+$ frequency values in each dot plot. It should be noted that identical results were obtained when the fluorochromes of HLA tetramers were reversed. *B*, PBMCs of Pt-03 taken at several different time points were stained with HLA-B*35 tetramer in complex with the Arg^{75} (RPQVPLRPMTY) or Thr^{75} (TPQVPLRPMTY) Nef peptide and subsequently with anti-CD8 mAb and 7-AAD. The frequency of $tetramer^+CD8^+$ in the total $CD8^+$ subset was calculated and plotted in the graph.

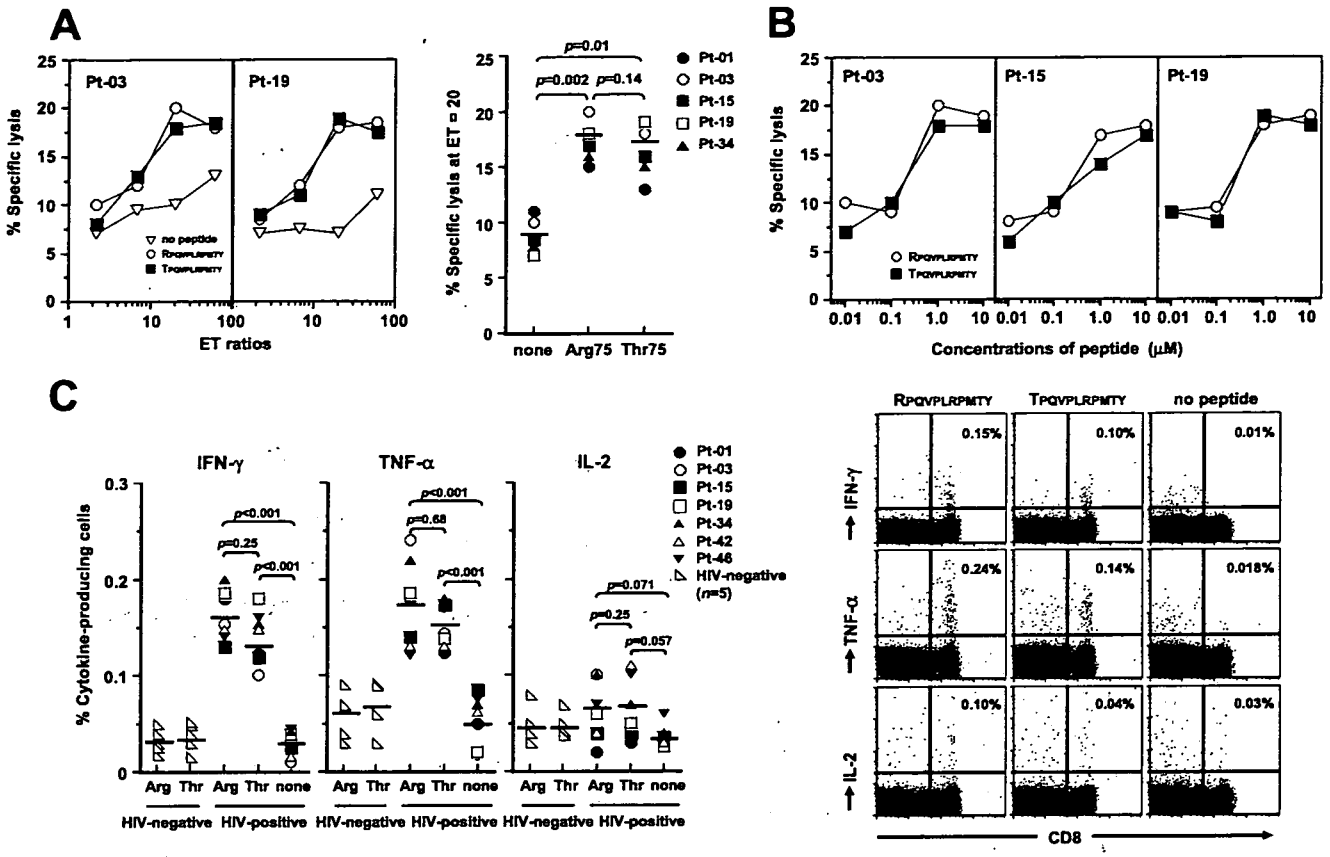

FIGURE 4. Antiviral effector functions of CD8 T cells specific for Nef epitopes. *A*, The cytotoxic activity of $CD8^+$ cells isolated from PBMC samples of HIV-positive donors (Pt-01, Pt-03, Pt-15, Pt-19, and Pt-34) was examined by ^{51}Cr-release assay directly ex vivo. The autologous target cells alone or pulsed with 1 μM Arg^{75} or Thr^{75} peptide were incubated with the effector $CD8^+$ cells at E:T ratios of 2.2, 6.7, 20, and 60 for 12 h. At the *left*, a representative set of data for Pt-03 and Pt-19 is shown. At the *right*, cytotoxic activity obtained at an E:T ratio of 20 is shown. Horizontal bars in the graphs indicate the mean for each group. It should be noted that the cytotoxic activity of $CD8^+$ cells was not examined for Pt-42 and Pt-46 because of the insufficient number of cells available for this assay. *B*, The cytotoxic activity of $CD8^+$ cells isolated from PBMC samples of HIV-positive donors (Pt-03, Pt-15, and Pt-19) was examined by the ^{51}Cr-release assay with the autologous target cells pulsed with the indicated concentrations of the Arg^{75} or Thr^{75} peptide at an E:T ratio of 20. Specific lysis in the absence of peptide is shown in *A*. *C*, PBMC samples, the same as those used in Fig. 1*A*, were stimulated or unstimulated with 1 μM Arg^{75} or Thr^{75} peptide for 6 h and then stained intracellularly with anti-IFN-γ, TNF-α, or IL-2 mAbs. The frequencies of the subsets exhibiting cytokine$^+CD8^+$ cells within the $CD8^+$ cell population are indicated in the graphs. Horizontal bars in the graphs indicate the mean for each group. At the *right* a representative set of dot plots for Pt-03 is shown with cytokine$^+$ frequency values at the *upper right corner* of each dot plot.

Thr^{75} (Table I), suggesting a lack of Thr^{75}-specific T cell precursors due to original antigenic sin or a lack of proliferation capacity in these subjects.

HLA tetramer analysis of CD8 T cells specific for Nef and its variant ex vivo

To see whether the Thr^{75} variant epitope was recognized by CD8 T cells, we obtained PBMC samples from seven chronically infected patients (Table I) after the variant viruses had become dominant and analyzed them ex vivo by using HLA tetramers. The frequencies of the RPQVPLRPMTY-B35 and TPQVPLRPMTY-B35 tetramer$^+$ subsets within the $CD8^+$ cells of the seven HIV-infected patients were significantly above the background level, being 0.261 ± 0.094 and 0.186 ± 0.081%, respectively; whereas those of five HIV-negative donors were 0.015 ± 0.0045 and 0.018 ± 0.009%, respectively (Fig. 3*A*). The frequencies of the cross-reactive fractions were <0.02% in all samples tested (Fig. 3*A*). These data indicate that the Thr^{75} and Arg^{75} peptides were immunogenic and exclusively recognized by a different subset of CD8 T cells widely in chronic HIV-infected patients having HLA-B*35.

Longitudinal analysis of Pt-03 PBMC showed that the CD8 T cells specific for the Arg^{75} peptide decreased in frequency and those specific for the Thr^{75} peptide increased (Fig. 3*B*). The increase in the frequency of Thr^{75}-specific CD8 T cells appeared to occur following the dominance of the Thr^{75} variant over the autologous virus (Table I). However, the question of whether Thr^{75}-specific CD8 T cells were absent before the autologous virus developed the Thr^{75} mutation could not be examined because PBMC samples during the primary infection were not available in this study. However, considering the following three points, namely that Thr^{75} (22 of 390; 5.6%) was rarely found in the Los Alamos database compared with Arg^{75} (302 of 390; 77.4%), the autologous virus from five of seven patients developed the Arg to Thr mutation during chronic infection (Table I), and cross-reactive CD8 T cell subsets were barely found in all subjects, it is most likely that Thr^{75}-specific CD8 T cells were newly generated in vivo in response to the Thr^{75} epitope after the autologous virus had undergone the Thr^{75} mutation.

Cytotoxic activity of CD8 T cells specific for Nef and its variant ex vivo

We then examined the Arg^{75}- or Thr^{75}-specific CD8 T cells for their Ag-specific killing activity. Because the variant Thr^{75}-specific CTL lines or clones could not be established in vitro (Fig. 2*A*) although the Thr^{75}-specific CD8 T cells were found ex vivo by the

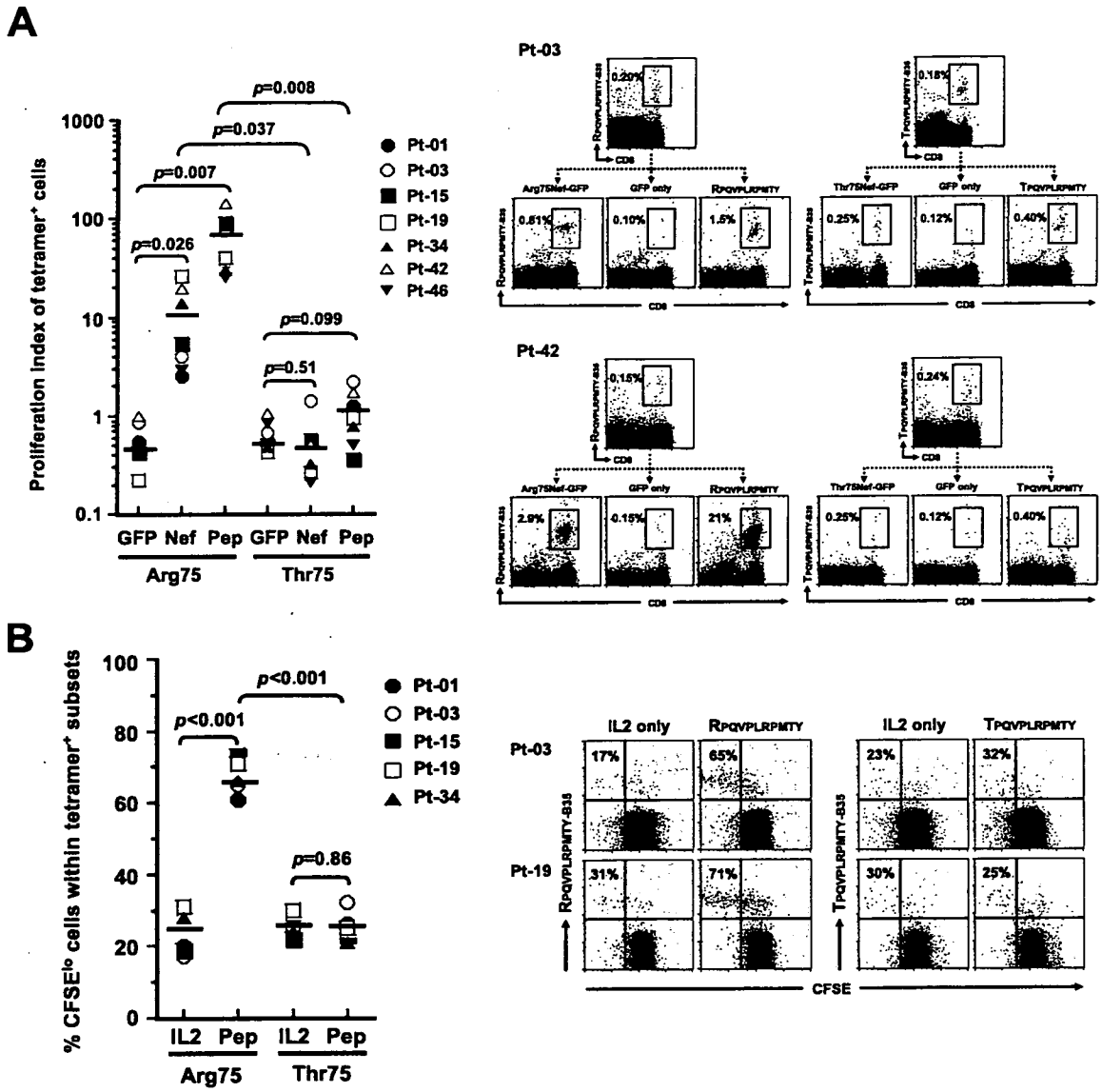

FIGURE 5. Proliferative capacity of CD8 T cells specific for Nef epitopes. *A*, The PBMC samples, the same as those used in Fig. 1*A*, were stimulated with irradiated C1R-B*3501 cells or autologous EBV-transformed B cells that had been pulsed with 1 μM Arg^{75} or Thr^{75} peptide or had been transduced with mRNA encoding GFP or Nef-GFP fusion proteins carrying Arg^{75} or Thr^{75}. Twelve days after the stimulation, the cells were analyzed with the HLA-B*35 tetramers. As shown in the graph at the *left*, the proliferation index was obtained as the ratio of tetramer$^+$ frequencies after and before stimulation. Horizontal bars in the graphs indicate the mean for each group. At the *right*, a representative set of dot plots for Pt-03 and Pt-42 is shown with tetramer$^+$ frequency values. *B*, The PBMC samples of HIV-positive donors (Pt-01, Pt-03, Pt-15, Pt-19, and Pt-34) were first labeled with CFSE and incubated in a medium containing human rIL-2 (100 U/ml). The cells were stimulated with IL-2 alone or in combination with 1 μM Arg^{75} or Thr^{75} peptide. After 6 days of culture, the cells were then stained with indicated HLA-tetramers and anti-CD8 and -CD3 Abs. The $CD3^+$ $CD8^+$ subsets were gated and analyzed for their fluorescence intensity of CFSE. The frequency of $CFSE^{low}$ cells within the tetramer$^+$ subset is shown in the graph at the *left*. Horizontal bars in the graph indicate the mean for each group. At the *right*, a representative set of dot plots for Pt-03 and Pt-19 is shown with $CFSE^{low}$ frequency values. It should be noted that CFSE dilution assay was not conducted for the subjects Pt-42 and Pt-46 because of the insufficient number of cells available for this assay.

tetramer analysis (Fig. 3*A*), we sought to analyze the Ag-specific cytolytic activity of CD8 T cells by a ^{51}Cr-release assay directly ex vivo. $CD8^+$ and $CD8^-$ cells were first isolated from the PBMCs of HIV-positive donors by a magnetic bead separation system and used as effector and target cells, respectively, for the cytolytic assay. The $CD8^+$ cells of the subjects tested showed cytotoxic to target cells pulsed with Arg^{75} and Thr^{75} peptides (1 μM) at an E:T ratio of 20 with specific lysis of 17.2 ± 1.9% and 16.2 ± 2.4%, respectively (Fig. 4*A*), whereas the background level of their specific lysis in the absence of the peptide was 8.9 ± 1.6% (Fig. 4*A*). As also shown in the representative data for Pt-03 and Pt-19 with various E:T ratios, the cytolytic activity of $CD8^+$ cells specific for the Arg^{75} and Thr^{75} peptides was not substantially different (Fig. 4*A*).

Peptide titration experiments were also performed using $CD8^+$ cells of Pt-03, Pt-15, and Pt-19, as these subjects showed relatively high cytolytic activity ex vivo (Fig. 4*A*). As shown in Fig. 4*B*, the cytolytic activity of $CD8^+$ cells toward cells pulsed with the Arg^{75} and Thr^{75} peptides was not much different in any range of the peptide concentration tested, suggesting the comparable functional avidity of both CD8 T cell subsets toward the given Ag.

Production of antiviral cytokines of CD8 T cells specific for Nef and its variant ex vivo

We further examined the ability of Nef-specific CD8 T cells to produce antiviral cytokines. The data show that IFN-γ and TNF-α responses were all significantly above the background level, being

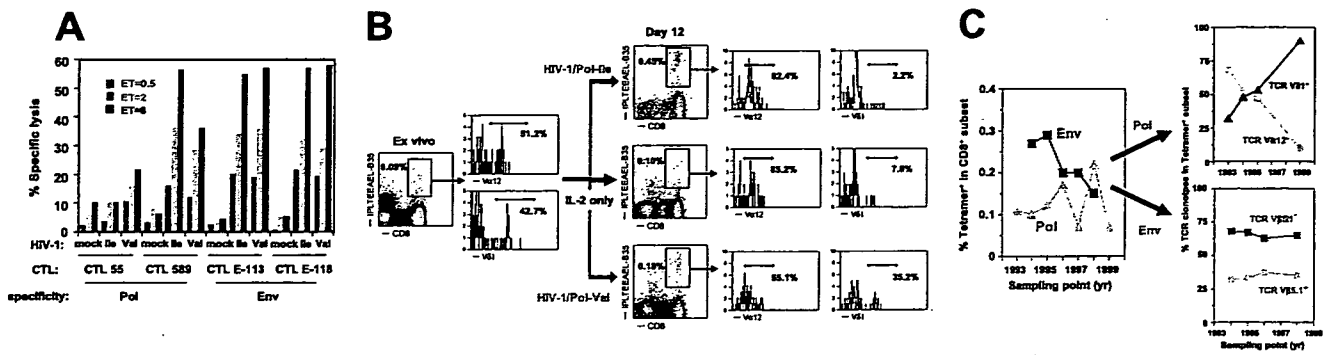

FIGURE 6. Functional analysis of CD8 T cells specific for Pol and Env epitopes. *A*, Cytotoxic activity of four different CTL clones, CTL 55, CTL 589, E-113, and E-118, toward autologous EBV-transformed B cells infected with mock or vesicular stomatitis virus envelope glycoprotein-pseudotyped HIV-1 expressing Ile or Val at Pol 448. It should be noted that ~75% of the target cells were positive for p24 Gag protein expression. *B*, Pt-03 PBMCs were stimulated with IL-2 alone or with autologous EBV-transformed B cells infected with the same viruses as above. After 12 days in culture, the cells were stained with a HLA-B*35 tetramer in complex with Pol-Ile peptide and then additionally with anti-CD8 and anti-TCR mAbs. The $CD8^+$ $tetramer^+$ subsets were gated and analyzed for their TCR usage. *C*, PBMCs of Pt-03 taken at several different time points were separately stained with the HLA-B*35 tetramer in complex with the Pol (IPLTEEAEL) or Env (DPNPQEVVL) peptide and subsequently with anti-CD8 and anti-TCR mAbs. The $CD8^+$$tetramer^+$ subsets were gated and analyzed for their TCR usage.

0.161 ± 0.025 and 0.171 ± 0.047%, respectively, in response to the Arg^{75} peptide and 0.140 ± 0.027 and 0.150 ± 0.023%, respectively, in response to the Thr^{75} peptide (Fig. 4*B*). In contrast, the IL-2 response was not significant, being 0.061 ± 0.031 and 0.063 ± 0.031% in response to the Arg^{75} and Thr^{75} peptides, respectively (Fig. 4*B*). Also, the extent of generation of cytokine-producing cells (IFN-γ and TNF-α) in response to Arg^{75} and Thr^{75} peptides was not significantly different (Fig. 4*B*), indicating that CD8 T cells specific for the Arg^{75} and Thr^{75} peptides were comparably functional in terms of Ag-specific cytokine production.

Proliferation capacity of CD8 T cells specific for Nef and its variant ex vivo

We next tested the Nef-specific CD8 T cells for their Ag-specific proliferation capacities ex vivo as assessed by both the expansion of $tetramer^+$ cells and the dilution of CFSE fluorescence intensity, because recent reports showed that HIV-specific CD8 T cells with progressive infection lose their ability to proliferate in response to Ag (3, 4).

PBMC samples were mixed with autologous EBV-transformed B cell lines or C1R-B*3501 cells expressing GFP or Nef-GFP fusion proteins carrying Arg^{75} or Thr^{75} in the absence or presence of the synthetic Arg^{75} or Thr^{75} peptide, respectively, and then analyzed by using HLA tetramers on days 0, 6, and 12. Because continuous expansion was observed even between days 6 and 12 (data not shown), the proliferation index was calculated by dividing the frequency of $tetramer^+$ cells at day 12 after stimulation with a given Ag by the frequency of $tetramer^+$ cells ex vivo (Fig. 5*A*). We considered a proliferation index of <1.0 to indicate no proliferation capacity of the subset. All subjects tested showed significant expansion of Arg^{75}-specific CD8 T cells upon stimulation with Arg^{75}-Nef-GFP and the Arg^{75} peptide with an index value of 11.4 ± 7.11 and 62.4 ± 41.9, respectively, whereas they did not show Ag-specific expansion upon stimulation with GFP alone, Thr^{75}-Nef-GFP, or the Thr^{75} peptide because the index value was 0.635 ± 0.166, 0.554 ± 0.279 or 1.11 ± 0.66, respectively (Fig. 5*A*). Also, the proliferation index of untreated PBMC (IL-2 alone) was 0.742 ± 0.203 (data not shown).

To further confirm the difference in proliferative capacity between Arg^{75}- and Thr^{75}-specific CD8 T cells, we analyzed them by monitoring CFSE fluorescence of $tetramer^+$ cells upon stimulation with the cognate peptides for 6 days. Upon stimulation with IL-2 alone, the frequencies of proliferating cells as measured by $CFSE^{low}$ cells within the $tetramer^+$ cells were 23.0 ± 6.1 and 25.8 ± 3.2% for Arg^{75} and Thr^{75}-specific cells, respectively (Fig. 5*B*). Stimulation with the Arg^{75} peptide resulted in a significant increase of proliferating CD8 T cells specific for the Arg^{75} peptide, as the frequency of $CFSE^{low}$ cells within the $tetramer^+$ cells was 67.2 ± 4.8% (Fig. 5*B*). In contrast, the Thr^{75} peptide stimulation showed virtually no change in the frequency of $CFSE^{low}$ cells within the $tetramer^+$ cells (25.4 ± 4.1%) compared with stimulation with IL-2 alone (Fig. 5*B*). Thus, the proliferative capacity of CD8 T cell subsets obtained by a CFSE dilution assay (Fig. 5*B*) was in good agreement with the data obtained by quantification of the $tetramer^+$ cell expansion assay (Fig. 5*A*). These data indicate that CD8 T cells specific for the Arg^{75} peptide retained their Ag-dependent proliferative capacity in patients with chronic HIV-1 infection, whereas those specific for the variant Thr^{75} peptide did not have such capacity (Fig. 5, *A* and *B*) although both cells showed comparable Ag-specific cytolytic activity (Fig. 4*A*) and cytokine secretion activity (Fig. 4*B*). Also, this observation may explain the failure to generate CTL clones or lines specific for the Thr^{75} peptide in vitro (see above).

Functional analysis of CTL clones specific for Pol, Env, and variant epitopes

Next we examined CD8 T cell responses to Pol, Env, and their variant epitopes. The binding activity between HLA-B*3501 and the wild-type (Pol-Ile; IPLTEEAEL) or the variant epitope (Pol-Val; VPLTEEAEL) was comparable, and analysis of Pt-03 PBMC with tetramers in complex with either peptide showed that all $tetramer^+$ cells were cross-reactive for both tetramers (data not shown) and that they consisted of two different clonotypes, $Vδ1^+$ and $Vα12^+$ (Table II). The representative clones, which had been generated by stimulation with the Pol-Ile peptide, were CTL55 (21) and CTL589 (18), respectively. CTL589 was cytotoxic toward cells infected with HIV-1 expressing Pol-Ile or Pol-Val ($HIV\text{-}1_{Pol\text{-}Ile}$ and $HIV\text{-}1_{Pol\text{-}Val}$, respectively), whereas CTL55 killed $HIV\text{-}1_{Pol\text{-}Val}$-infected cells but not $HIV\text{-}1_{Pol\text{-}Ile}$-infected cells (Fig. 6*A*), indicating that CTL55 was exclusively specific for the variant Pol-Val epitope in terms of virus-infected cells as a target.

TCR analysis of a number of CTL clones specific for the Env epitope generated from Pt-03 PBMCs revealed that they also consisted of two different TCR clonotypes (Table II). Representative CTL clones CTL E-113 and E-118 were comparably cytotoxic

toward cells infected with HIV-$1_{Pol\text{-}Ile}$ or HIV-$1_{Pol\text{-}Val}$ (Fig. 6*A*), suggesting no functional difference between Env-specific CTLs. Taken together, the data suggest that differential functional cytotoxicity of CTL clonotypes toward wild-type and variant HIV-1 was caused by antigenic variations of the Pol epitope in autologous HIV-1.

Impaired proliferation of CD8 T cells specific for the Pol variant epitope ex vivo

We then tested the Pol-specific CD8 T cells for their proliferation activity in response to HIV-$1_{Pol\text{-}Ile}$ and HIV-$1_{Pol\text{-}Val}$ ex vivo. Pt-03 PBMCs were cocultured with cells infected with mock (IL-2 alone), HIV-$1_{Pol\text{-}Ile}$, or HIV-$1_{Pol\text{-}Val}$ for 12 days and then stained with HLA-B35 tetramers. The proliferation index of the $V\alpha12^+$tetramer$^+$ subset was ~10, 2, and 1 when the cells were stimulated with HIV-$1_{Pol\text{-}Ile}$, HIV-$1_{Pol\text{-}Val}$, and IL-2 alone, respectively (Fig. 6*B*), indicating that the $V\alpha12^+$ CD8 T cells had potent proliferation activity in response to the Pol-Ile epitope. However, the proliferation index of the $V\delta1^+$ tetramer$^+$ subset was <1.5 in response to both viruses (Fig. 6*B*), indicating the impaired Ag-specific proliferation of this subset of CD8 T cells specific for the variant Pol-Val epitope. Thus, not only CD8 T cells specific for the variant Nef epitope but also those specific for the variant Pol epitope showed impaired Ag-specific proliferation activity ex vivo (Figs. 5, *A* and *B*, and 6*B*).

Finally, we longitudinally analyzed the changes in tetramer$^+$ frequencies specific for Pol and Env epitopes and their constituent T cell clonotypes of subject Pt-03. TCR clonotypes within the Pol-specific CD8$^+$ cell population showed an increase in the frequency of the functionally impaired $V\delta1^+$ subset over time (Fig. 6*C*), suggesting that the sum of antiviral effector functions of Pol-specific CD8 T cells had declined. The time course of this change seemed to have occurred after the appearance of the Ile to Val mutation in the autologous HIV-1 (Table I). In contrast, an analysis of the Env-specific CD8 T cell response revealed that the frequency of the $V\beta5(c)^+$ T cell clonotypes within the Env-specific tetramer$^+$ subset was virtually constant (Fig. 6*C*). These data suggest that T cell clonotypes within the same specificity had not basically changed over time in the absence of significant variations within the epitope, thus highlighting the substantial changes in specificity and clonotypes observed in CD8 T cells specific for Pol and Nef epitopes with mutations at TCR contact sites.

Discussion

We showed herein that the CTL escape mutations that abolished TCR recognition had the ability to recruit variant-specific CTLs using different TCR clonotypes after the autologous HIV-1 had become dominated by the variant during the chronic phase of an HIV-1 infection in patients with HLA-B*35. However, because these variant-specific CTLs did not have potent Ag-specific proliferation capacity, this recruitment of CTLs barely correlated with the increased antiviral effectiveness of HIV-specific CTLs, although the breadth or magnitude of HIV-specific CTL responses was apparently maintained. Thus, these data demonstrate that CTL escape mutations that abolished TCR recognition not only led to escape from established wild-type-specific CTL responses but also could eventually have the additional effect of generating variant-specific CTLs with impaired proliferative capacity. Apparently, this observation provides evidence that supports the paradigm in CTL escaplogy in which CTL escape virus variants can persist only if the host is unable to mount an immune response against the variant epitopes or if the newly generated variant-specific immune responses are not as effective as the established wild type-specific ones.

It has recently been reported that the functional heterogeneity and loss of proliferative activity of virus-specific CD8 T cell responses is influenced by Ag persistence and Ag levels in mice and humans (5–7). The data obtained in this study showing a loss of proliferative capacity of variant-specific CTLs despite their having an IFN-γ-producing activity are surprisingly similar to those data showing virus-specific CTLs functionally impaired by chronic Ag exposure in mice chronically infected with the lymphocytic choriomeningitis virus (6). Thus, our data can be interpreted to indicate that when the CTL escape virus variants become dominant, the variant-specific CD8 T cells are repeatedly stimulated by the variant Ags, which can lead to a loss of functions by the variant-specific subsets, whereas the wild type-specific CD8 T cells see little Ag, which can lead to the restoration of functions by the wild type-specific ones. In this regard, it is interesting to ask whether CD8 T cells specific for the wild-type and the variant Nef epitopes differently express a receptor programmed death 1 (PD-1), because several recent reports show that functionally impaired virus-specific CD8 T cells express PD-1 in mice and humans chronically infected with lymphocytic choriomeningitis virus (8) and HIV-1 (23, 24), respectively. However, we observed no significant difference in the level of PD-1 expression between CD8 T cells specific for the wild-type and variant Nef epitopes or even for other epitopes in this setting (data not shown), most likely because only a limited number of subjects was tested or the subjects tested had been receiving antiretroviral therapy in this study. Because relatively large variations were demonstrated in the level of PD-1 expression in virus-specific human CD8 T cells among individuals and specificities within the same individual and because antiretroviral therapy also influenced PD-1 expression (23, 24), it could be difficult to estimate the level of functional impairment of CD8 T cells from the absolute level of PD-1 expression when a limited number of subjects and epitopes are tested. Further studies are needed to clarify the effect of antigenic variations of HIV-1 on the differential levels of PD-1 expression in HIV-1-specific CD8 T cells in untreated subjects with acute and chronic phase of HIV-1 infection.

Alternatively, a report showing the restoration of a proliferative response by some fractions of HIV-specific CD8 T cells through the addition of exogenous IL-2 highlights the importance of IL-2-secreting CD4 helper T cells for the maintenance of effective antiviral CD8 T cell responses in a chronic infection (4). Another report showing that HIV-specific CD8 T cell proliferation is supported by IL-2-secreting CD8 T cells in vitro suggests the importance of autocrine help to maintain CD8 T cell effectiveness during the CD4-diminished chronic phase of an infection (5). In our study, the difference in the proliferative capacity of CD8 T cells in patients with a chronic infection was primarily related to their epitope specificity. CD8 T cells specific for the variant epitopes had diminished proliferative capacity even in the presence of exogenous IL-2. Considering that the variant epitopes were selected and became dominant late after the primary infection, it is possible that the variant-specific CD8 T cells could have been primed during the CD4-diminished chronic phase of infection, resulting in impaired function of the variant-specific CD8 T cells.

It is also thought that wild-type and variant epitopes have a different inherent property for inducing CD8 T cell responses, as the nature of the Ags determines helper requirement for CTL priming in vivo (25). The variant-specific CTLs may not be fully functional due to the low avidity interactions between their TCRs and the variant Ags. Indeed, the variant Pol-specific CTL clone (CTL55) showed weak killing activity toward cells infected with the variant virus in our study, suggesting the generation of low avidity CD8 T cells in response to antigenic variations of the virus.

However, this was not the case in the Nef-specific CD8 T cells, as a cytolytic assay ex vivo showed that wild-type and variant Nef-specific CD8 T cells had comparable functional avidity in our study, suggesting that the variant epitope has immunogenic potential sufficient for CTL recognition, although the newly arising variant-specific CD8 T cells showed impaired proliferative capacity. Given that such a variant epitope is potentially immunogenic, it is possible that the variant Ag could induce fully functional CTL responses when individuals are primary infected with the variant virus. This issue needs to be further addressed as such information will be important for therapeutic vaccine design.

Original antigenic sin, which was originally described in the humoral response to influenza virus, has been applied to cellular responses for limiting the ability of the immune system to generate new responses to escape variants (26, 27). In this scenario, variant-specific CTLs are not generated but the variant epitope can continue to stimulate the proliferation of CTLs specific for the wild-type epitope (28). In our study, the ex vivo analysis of patients' PBMCs by HLA tetramers as well as IFN-γ assays clearly showed the generation of CD8 T cells exclusively specific for the variant epitopes, indicating that original antigenic sin could be overcome in the case of some HLA-B*35-restricted epitopes. This finding is consistent with recent reports showing that, based on ex vivo analysis by IFN-γ assays, the human immune system is capable of mounting novel CD8 T cell responses against CTL escape variants of Gag epitopes restricted by HLA-A*11 (29) and HLA-B*57 (30). However, considering that *HLA-B*35* is an HLA class I allele associated with rapid disease progression while *HLA-A*11* and *HLA-B*57* are associated with slow disease progression (10, 31), it is conceivable that the failure to generate functionally effective, variant-specific CTLs restricted by HLA-B*35, as observed in this study, could result in relatively insufficient virus containment by HLA-B*35-restricted CTL responses in vivo, leading to a consequent association between *HLA-B*35* and rapid disease progression. In this regard, further comprehensive analysis of the wild-type and variant-specific CTL responses restricted by HLA-B*35 and certain B*35 subtypes in treatment-naive subjects is becoming intriguing.

It is of note that the frequency of the wild type Pol-specific CD8 T cell subsets was much reduced after the emergence of CTL escape variants in the Pol epitope, whereas the wild type Nef-specific ones persisted following CTL escape in the Nef epitope in our study. Because we obtained autologous virus sequence data from viral RNAs in plasma, it is conceivable that a small number of cells latently infected with the variant viruses yet having a wild-type Nef sequence remained in vivo and eventually reactivated the wild type Nef-specific CD8 T cell subsets. Alternatively, a transient reversion of variant viruses to the wild-type Nef sequence arose, although such wild-type viruses could be rapidly controlled by wild type-specific CD8 T cells to undetectable levels. In any event, these scenarios can be possible when a virus variant has replicative disadvantage over the wild-type virus in vivo. Interestingly, it is reported (32) that the Thr mutation in Nef (corresponding to Thr^{75} in this study although a different numbering system was used therein) resulted in much decreased capacity for supporting viral replication, although the replication-competent strain NL43 has Thr at the same position. Further analysis to clarify whether CTL-mediated selective pressure can modulate the pathogenic functions of Nef and lead to long-term favorable effects on HIV-infected individuals against disease progression would be intriguing.

Recent studies have demonstrated that mutational escape from HIV-specific CTL is caused by interference with the intracellular processing of virus-derived proteins (15, 16). We also found HLA-B*35-associated mutations flanking the epitopic regions in Env and Nef. However, Env-specific CTL clones showed comparable cytolytic activity toward cells expressing wild-type and mutant proteins (T. Ueno, unpublished observations), suggesting that altered Ag processing was not involved in this setting. Further studies are needed to determine whether and, if so, how antigenic variations causing altered Ag processing affect HLA-B*35-restricted CTL responses and the functional heterogeneity of HIV-specific CTLs in patients with a chronic infection.

Acknowledgments

We thank Drs. H. Tomiyama and A. Kawana-Tachikawa for helpful discussion, and S. Douki for technical help.

Disclosures

The authors have no financial conflict of interest.

References

1. Addo, M. M., X. G. Yu, A. Rathod, D. Cohen, R. L. Eldridge, D. Strick, M. N. Johnston, C. Corcoran, A. G. Wurcel, C. A. Fitzpatrick, et al. 2003. Comprehensive epitope analysis of human immunodeficiency virus type 1 (HIV-1)-specific T-cell responses directed against the entire expressed HIV-1 genome demonstrate broadly directed responses, but no correlation to viral load. *J. Virol.* 77: 2081–2092.
2. Betts, M. R., D. R. Ambrozak, D. C. Douek, S. Bonhoeffer, J. M. Brenchley, J. P. Casazza, R. A. Koup, and L. J. Picker. 2001. Analysis of total human immunodeficiency virus (HIV)-specific $CD4^+$ and $CD8^+$ T-cell responses: relationship to viral load in untreated HIV infection. *J. Virol.* 75: 11983–11991.
3. Migueles, S. A., A. C. Laborico, W. L. Shupert, M. S. Sabbaghian, R. Rabin, C. W. Hallahan, D. Van Baarle, S. Kostense, F. Miedema, M. McLaughlin, L. Ehler, J. Metcalf, S. Liu, and M. Connors. 2002. HIV-specific $CD8^+$ T cell proliferation is coupled to perforin expression and is maintained in nonprogressors. *Nat. Immunol.* 3: 1061–1068.
4. Lichterfeld, M., D. E. Kaufmann, X. G. Yu, S. K. Mui, M. M. Addo, M. N. Johnston, D. Cohen, G. K. Robbins, E. Pae, G. Alter, et al. 2004. Loss of HIV-1-specific $CD8^+$ T cell proliferation after acute HIV-1 infection and restoration by vaccine-induced HIV-1-specific $CD4^+$ T cells. *J. Exp. Med.* 200: 701–712.
5. Zimmerli, S. C., A. Harari, C. Cellerai, F. Vallelian, P.-A. Bart, and G. Pantaleo. 2005. HIV-1-specific IFN-γ/IL-2-secreting CD8 T cells support CD4-independent proliferation of HIV-1-specific CD8 T cells. *Proc. Natl. Acad. Sci. USA* 102: 7239–7244.
6. Wherry, E. J., D. L. Barber, S. M. Kaech, J. N. Blattman, and R. Ahmed. 2004. Antigen-independent memory CD8 T cells do not develop during chronic viral infection. *Proc. Natl. Acad. Sci. USA* 101: 16004–16009.
7. Klenerman, P., and A. Hill. 2005. T cells and viral persistence: lessons from diverse infections. *Nat. Immunol.* 6: 873–879.
8. Barber, D. L., E. J. Wherry, D. Masopust, B. Zhu, J. P. Allison, A. H. Sharpe, G. J. Freeman, and R. Ahmed. 2006. Restoring function in exhausted CD8 T cells during chronic viral infection. *Nature* 439: 682–687.
9. Migueles, S. A., M. S. Sabbaghian, W. L. Shupert, M. P. Bettinotti, F. M. Marincola, L. Martino, C. W. Hallahan, S. M. Selig, D. Schwartz, J. Sullivan, and M. Connors. 2000. HLA B*5701 is highly associated with restriction of virus replication in a subgroup of HIV-infected long term nonprogressors. *Proc. Natl. Acad. Sci. USA* 97: 2709–2714.
10. O'Brien, S. J., X. Gao, and M. Carrington. 2001. HLA and AIDS: a cautionary tale. *Trends Mol. Med.* 7: 379–381.
11. Dong, T., G. Stewart-Jones, N. Chen, P. Easterbrook, X. Xu, L. Papagno, V. Appay, M. Weekes, C. Conlon, C. Spina, et al. 2004. HIV-specific cytotoxic T cells from long-term survivors select a unique T cell receptor. *J. Exp. Med.* 200: 1547–1557.
12. Ueno, T., H. Tomiyama, M. Fujiwara, S. Oka, and M. Takiguchi. 2004. Functionally impaired HIV-specific CD8 T cells show high affinity TCR-ligand interactions. *J. Immunol.* 173: 5451–5457.
13. Goulder, P. J. R., and D. I. Watkins. 2004. HIV and SIV CTL escape: implications for vaccine design. *Nat. Rev. Immunol.* 4: 630–640.
14. Moore, C. B., M. John, I. R. James, F. T. Christiansen, C. S. Witt, and S. A. Mallal. 2002. Evidence of HIV-1 adaptation to HLA-restricted immune responses at a population level. *Science* 296: 1439–1443.
15. Yokomaku, Y., H. Miura, H. Tomiyama, A. Kawana-Tachikawa, M. Takiguchi, A. Kojima, Y. Nagai, A. Iwamoto, Z. Matsuda, and K. Ariyoshi. 2004. Impaired processing and presentation of cytotoxic-T-lymphocyte (CTL) epitopes are major escape mechanisms from CTL immune pressure in human immunodeficiency virus type 1 infection. *J. Virol.* 78: 1324–1332.
16. Draenert, R., S. Le Gall, K. J. Pfafferott, A. J. Leslie, P. Chetty, C. Brander, E. C. Holmes, S.-C. Chang, M. E. Feeney, M. M. Addo, et al. 2004. Immune selection for altered antigen processing leads to cytotoxic T lymphocyte escape in chronic HIV-1 infection. *J. Exp. Med.* 199: 905–915.
17. Kawana, A., H. Tomiyama, M. Takiguchi, T. Shioda, T. Nakamura, and A. Iwamoto. 1999. Accumulation of specific amino acid substitutions in HLA-B35-restricted human immunodeficiency virus type 1 cytotoxic T lymphocyte epitopes. *AIDS Res. Hum. Retroviruses* 15: 1099–1107.

18. Ueno, T., H. Tomiyama, and M. Takiguchi. 2002. Single T cell receptor-mediated recognition of an identical HIV-derived peptide presented by multiple HLA class I molecules. *J. Immunol.* 169: 4961–4969.
19. Lefranc, M. P., V. Giudicelli, Q. Kaas, E. Duprat, J. Jabado-Michaloud, D. Scaviner, C. Ginestoux, O. Clement, D. Chaume, and G. Lefranc. 2005. IMGT, the international ImMunoGeneTics information system. *Nucleic Acids Res.* 33: D593–D597.
20. Akari, H., S. Arold, T. Fukumori, T. Okazaki, K. Strebel, and A. Adachi. 2000. Nef-induced major histocompatibility complex class I down-regulation is functionally dissociated from its virion incorporation, enhancement of viral infectivity, and CD4 down-regulation. *J. Virol.* 74: 2907–2912.
21. Ueno, T., H. Tomiyama, M. Fujiwara, S. Oka, and M. Takiguchi. 2003. HLA class I-restricted recognition of an HIV-derived epitope peptide by a human T cell receptor α chain having a Vδ1 variable segment. *Eur. J. Immunol.* 33: 2910–2916.
22. Casazza, J. P., M. R. Betts, B. J. Hill, J. M. Brenchley, D. A. Price, D. C. Douek, and R. A. Koup. 2005. Immunologic pressure within class I-restricted cognate human immunodeficiency virus epitopes during highly active antiretroviral therapy. *J. Virol.* 79: 3653–3663.
23. Trautmann, L., L. Janbazian, N. Chomont, E. A. Said, S. Gimmig, B. Bessette, M.-R. Boulassel, E. Delwart, H. Sepulveda, R. S. Balderas, et al. 2006. Upregulation of PD-1 expression on HIV-specific CD8$^+$ T cells leads to reversible immune dysfunction. *Nat. Med.* 12: 1198–1202.
24. Day, C. L., D. E. Kaufmann, P. Kiepiela, J. A. Brown, E. S. Moodley, S. Reddy, E. W. Mackey, J. D. Miller, A. J. Leslie, C. DePierres, et al. 2006. PD-1 expression on HIV-specific T cells is associated with T-cell exhaustion and disease progression. *Nature* 443: 350–354.
25. Franco, A., D. A. Tilly, I. Gramaglia, M. Croft, L. Cipolla, M. Meldal, and H. M. Grey. 2000. Epitope affinity for MHC class I determines helper requirement for CTL priming. *Nat. Immunol.* 1: 145–150.
26. Klenerman, P., and R. M. Zinkernagel. 1998. Original antigenic sin impairs cytotoxic T lymphocyte responses to viruses bearing variant epitopes *Nature* 394: 482–485.
27. Mongkolsapaya, J., W. Dejnirattisai, X. Xu, S. Vasanawathana, N. Tangthawornchaikul, A. Chairunsri, S. Sawasdivorn, T. Duangchinda, T. Dong, S. Rowland-Jones, et al. 2003. Original antigenic sin and apoptosis in the pathogenesis of dengue hemorrhagic fever. *Nat. Med.* 9: 921–927.
28. McAdam, S., P. Klenerman, L. Tussey, S. Rowland-Jones, D. Lalloo, R. Phillips, A. Edwards, P. Giangrande, A. Brown, and F. Gotch. 1995. Immunogenic HIV variant peptides that bind to HLA-B8 can fail to stimulate cytotoxic T lymphocyte responses. *J. Immunol.* 155: 2729–2736.
29. Allen, T. M., X. G. Yu, E. T. Kalife, L. L. Reyor, M. Lichterfeld, M. John, M. Cheng, R. L. Allgaier, S. Mui, N. Frahm, et al. 2005. De novo generation of escape variant-specific CD8$^+$ T-cell responses following cytotoxic T-lymphocyte escape in chronic human immunodeficiency virus type 1 infection. *J. Virol.* 79: 12952–12960.
30. Feeney, M. E., Y. Tang, K. Pfafferott, K. A. Roosevelt, R. Draenert, A. Trocha, X. G. Yu, C. Verrill, T. Allen, C. Moore, et al. 2005. HIV-1 viral escape in infancy followed by emergence of a variant-specific CTL response. *J. Immunol.* 174: 7524–7530.
31. Carrington, M., G. W. Nelson, M. P. Martin, T. Kissner, D. Vlahov, J. J. Goedert, R. Kaslow, S. Buchbinder, K. Hoots, and S. J. O'Brien. 1999. HLA and HIV-1: heterozygote advantage and B*35-Cw*04 disadvantage. *Science* 283: 1748–1752.
32. Fackler, O. T., D. Wolf, H. O. Weber, B. Laffert, P. D'Aloja, B. Schuler-Thurner, R. Geffin, K. Saksela, M. Geyer, and B. M. Peterlin. 2001. A natural variability in the proline-rich motif of Nef modulates HIV-1 replication in primary T cells. *Curr. Biol.* 11: 1294–1299.

HIV Medicine (2007), 8, 112–123

ORIGINAL RESEARCH

Predictors of CD4 count change over 8 months of follow up in HIV-1-infected patients with a CD4 count ≥ 300 cells/μL who were assigned to 7.5 MIU interleukin-2

The ESPRIT Research Group

Background

ESPRIT is a randomized trial comparing the clinical impact of interleukin (IL)-2 plus antiretrovirals vs antiretrovirals alone. Identification of factors that influence the relationship between IL-2 and CD4 count recovery will enable better personalization of treatment with IL-2 in HIV-1-positive individuals. The IL-2 induction phase consists of three dosing cycles over 6–8 months (7.5 MIU twice a day, for 5 days every 8 weeks).

Methods

We included patients initiating IL-2 at the 7.5 MIU dose with an 8-month CD4 count, measured at least 30 days after their last cycle. We identified baseline predictors of CD4 count changes over 8 months using linear regression.

Results

Of 2090 patients assigned IL-2, 1673 (80%) were included in the analysis. The median (interquartile range) baseline CD4 count was 461 (370, 587) cells/μL with a median increase of 233 (90, 411) cells/μL at month 8. After adjustments, significant predictors of CD4 count change included CD4 nadir (29.8 cells/μL greater increase per 100 cells/μL higher; $P<0.0001$), last CD4 count before baseline (mean 36.0 cells/μL greater increase per 100 cells/μL higher; $P<0.0001$), time from antiretroviral start to baseline (8.3 cells/μL smaller increase per year longer; $P=0.001$), age (11.7 cells/μL smaller increase per 5 years older; $P=0.005$) and race (79.7 cells/μL greater increase for black patients vs white patients; $P=0.003$). A linear relationship existed between total IL-2 dose in the first cycle and CD4 count change (73.1 cells/μL greater increase per 15 MIU higher; $P<0.0001$).

Conclusions

Prior nadir and current CD4 counts, age and IL-2 dose are major determinants of CD4 increases induced by with intermittent administration of IL-2 in HIV-1-positive individuals on antiretrovirals. The clinical function of these induced CD4 cells is under study.

Keywords: 7.5 MIU proleukin, CD4 cell count responses, subcutaneous recombinant interleukin-2

Received: 27 January 2006, accepted 19 October 2006

Introduction

The use of subcutaneous recombinant interleukin (IL)-2 (SC rIL-2), when given in conjunction with potent combination antiretroviral therapy (cART), produces significant and sustained increases in CD4 cell counts [1–7]. Studies that investigated rIL-2 doses from 1.5 million international units (MIU) to 7.5 MIU twice a day (bid) have shown that the gain in CD4 cell count associated with rIL-2 is dose related, with higher doses providing better responses [8–10]. As rIL-2 is a toxic cytokine it is not likely that a higher dose than 7.5 MIU will be tolerated, and therefore the 7.5 MIU bid dose is considered optimal.

The boost in peripheral blood CD4 cell counts induced by rIL-2 varies from person to person; some patients achieve substantial CD4 cell count increases whereas others simply do not respond at all [6]. Limited data are available on the characteristics of patients using cART who are likely to experience the greatest CD4 cell count responses from rIL-2. Previous findings, including those obtained in studies investigating IL-2 administration through different routes (e.g. pegylated or Continuous intravenous (CIV)),

Correspondence: Zoe Fox, CHIP, Hvidovre University Hospital, DK-2650 Hvidovre, Denmark. Tel: + 45 36 32 30 15; fax: + 45 36 47 33 40; e-mail: z.fox@pcps.ucl.ac.uk

suggest that predictors of response include age, HIV-RNA, CD4 cell count at start of IL-2 therapy and the CD4 nadir prior to starting IL-2 [11–13]. Four Vanguard trials were set up to identify the optimal dose of rIL-2 to use in Evaluation of Subcutaneous Proleukin in a Randomised International Trial (ESPRIT). Three of these trials were identically designed and showed marked regional differences in response rates after three cycles of rIL-2, with the Bangkok study exhibiting superior IL-2-induced CD4 cell count increases compared with either the Houston or Buenos Aires study at the 7.5 MIU bid dose, indicating possible racial and treatment management differences [10]. A racial difference was also observed in the US Vanguard study by Markowitz *et al.* [12]. Larger studies are required to confirm the validity of these predictors.

ESPRIT is a large international trial designed to assess the difference in the risk of clinical AIDS and death between patients randomized to antiretrovirals plus rIL-2 and those randomized to antiretrovirals alone. The trial is fully recruited and all patients have been followed for over 8 months, so the induction phase, which consists of three cycles of rIL-2 separated by at least 6 weeks, has been completed. Here we present an analysis of factors predicting CD4 cell count responses to rIL-2 after the induction phase in the largest patient group yet studied.

Methods

Study design

ESPRIT is an ongoing, international, phase III, open-label, randomized trial designed to evaluate the clinical impact of SC rIL-2 plus antiretroviral therapy (ART) vs ART alone. Four Vanguard studies were carried out before ESPRIT [7–10]. In three of these Vanguard studies (Bangkok, Buenos Aires and Houston), patients were randomized to no rIL-2 or rIL-2 at doses of 1.5, 4.5 or 7.5 MIU bid for 5 consecutive days (3 : 1 : 1 : 1, respectively) [10]. In the Vanguard study carried out by the Community Programs for Clinical Research on AIDS (CPCRA) [7], 511 patients were randomized to no rIL-2 or rIL-2 at doses of 4.5 or 7.5 MIU (2 : 1 : 1, respectively). All patients in Bangkok, Buenos Aires and Houston and 420 of the CPCRA patients were rolled over into ESPRIT [14].

Detailed information about the design of ESPRIT has been published elsewhere [1,14]. HIV-1-infected patients who had an absolute CD4 cell count ≥ 300 cells/μL in the 45 days prior to randomization and who were taking cART were eligible for enrolment. Patients had to be ≥ 18 years old and have bilirubin $\leq 2 \times$ upper limit of normal (ULN), creatinine ≤ 2.0 mg/dL and aspartate aminotransferase (AST) or alanine aminotransferase (ALT) levels $\leq 5 \times$ ULN in the 45 days prior to randomization. Exclusion criteria were prior IL-2 therapy; concurrent malignancy requiring cytotoxic chemotherapy; use of systemic corticosteroids, immunosuppressants, or cytotoxic agents within 45 days prior to randomization; current or historical autoimmune/inflammatory diseases; a central nervous system abnormality requiring treatment with antiseizure medication; a history of an AIDS-defining illness [Centers for Disease Control and Prevention (CDC) category C]; infection with a disease that is likely to be associated with immunodeficiency; pregnancy or breast feeding.

Laboratory methods and medication receipt

ESPRIT was conducted as an open-label study because it is impractical to use placebo injections and maintain blinding as a consequence of the side effects of rIL-2. All eligible patients, except Vanguard patients, were randomly assigned to no rIL-2 or SC rIL-2 with a dose of 7.5 MIU bid for 5 consecutive days. Patients were required to take ARTs over the 5 days of each dosing cycle. SC rIL-2 was to be given every 8 weeks for at least three cycles, with the initial cycle beginning within 2 weeks of randomization. Patients who commenced ARTs just prior to randomization must have been receiving them for at least 1 week before their first cycle of rIL-2. SC rIL-2 therapy was not to be given more frequently than every 6 weeks and, for the first three cycles, the maximum length of time between cycles was not to exceed 11 weeks. The initial three cycles of IL-2 are referred to as the induction phase.

Patients were monitored for dose-limiting side effects. Those experiencing a side effect were able to interrupt treatment or dose-reduce in decrements of 1.5 or 3.0 MIU per dose. Patients could have a maximum of two dose reductions during any one cycle. Minimum and maximum acceptable doses were 1.5 and 7.5 MIU bid, respectively.

Statistical analysis

This analysis investigates patients in the rIL-2 arm because the Data Safety monitoring Board (DSMB) recommended that data in the control arm (i.e. patients receiving ARTs without rIL-2) be kept blind. We restricted the analysis to patients starting rIL-2 at the 7.5 MIU bid dose because only a few patients started rIL-2 at lower doses. Patients using lower doses were mainly participants in the Vanguard studies, and findings for these studies have previously been reported [7,10,12]. Only patients who initiated rIL-2 attended their 8-month (± 2 months) visit and had an 8-month CD4 cell count at least 30 days after their most

recent rIL-2 cycle were included. This ensured enough time for the CD4 cell counts to stabilize after rIL-2 treatment.

Baseline and pre-baseline characteristics were examined and entered into a linear regression model to see if they were predictive of the change in CD4 cell counts after 8 months of follow up. CD4 cell counts in the 45 days prior to entry in addition to a maximum of three other CD4 cell counts in the year before entry were recorded at baseline; the mean CD4 cell count was calculated and the slope of decline was modelled using simple linear regression for individuals with at least three pre-baseline measurements.

Baseline covariates included in this analysis were HIV-RNA level ($\geq$ or $<$ 500 HIV-1 RNA copies/mL), gender, hepatitis B/C virus (HBV/HCV) status, CDC category, race, region (USA, South America, Asia, Australasia, South Europe, North Europe or Canada), mode of HIV-1 transmission, age, last CD4 cell count prior to baseline, CD4 cell percentage, CD4 cell count, CD4 nadir, slope of decline of CD4 count in the year prior to entry, time between start of ART and baseline, and body mass index. The last eight factors were treated as continuous variables and a linear relationship with CD4 cell count change was assumed. We checked the reasonableness of these assumptions using normal plots and graphs of fitted values against residuals.

If several baseline immunological markers were highly correlated and significantly associated with the outcome in single variable analyses, the marker for which the association with the outcome was most highly significant was identified and included in multivariable analysis to avoid problems associated with colinearity. The total rIL-2 dose received during the first cycle was also investigated through single variable analysis.

The baseline CD4 cell count was not included in the main model because it was used for calculating the outcome measure, i.e. the change in CD4 cell count from baseline. If it had been included, a spurious association would probably have been seen between the baseline value and the change from baseline because of a phenomenon known as 'regression towards the mean' [15,16]. Instead, to assess the effect of baseline CD4 cell count on the change at 8 months, we investigated the latest CD4 cell count prior to baseline. We included baseline CD4 cell count instead of CD4 cell count prior to baseline in a second model in order to understand its effect on the other predictors.

All covariates were entered into a multivariable model, but only variables that were still significant at the 5% level using a two-sided test were retained. Interactions between covariates were examined. All statistical analyses were performed using STATA software (STATA Statistical Software, version 8.2/SE; StataCorp, College Station, TX).

Results

Study population

Between November 2000 and April 2003, ESPRIT recruited 4150 individuals from 254 clinical sites in 25 countries. There were 2090 patients who were assigned SC rIL-2, and of these 1673 (80%) started rIL-2 at the 7.5 MIU bid dose and had an 8-month visit without a cycle in the 29 days preceding this visit. Of the 417 individuals who were excluded from these analyses, 179 were Vanguard patients randomly assigned to lower doses of rIL-2, 73 were assigned the 7.5 MIU dose but did not receive any, 8 took a lower dose than their assigned 7.5 MIU dose, 5 started

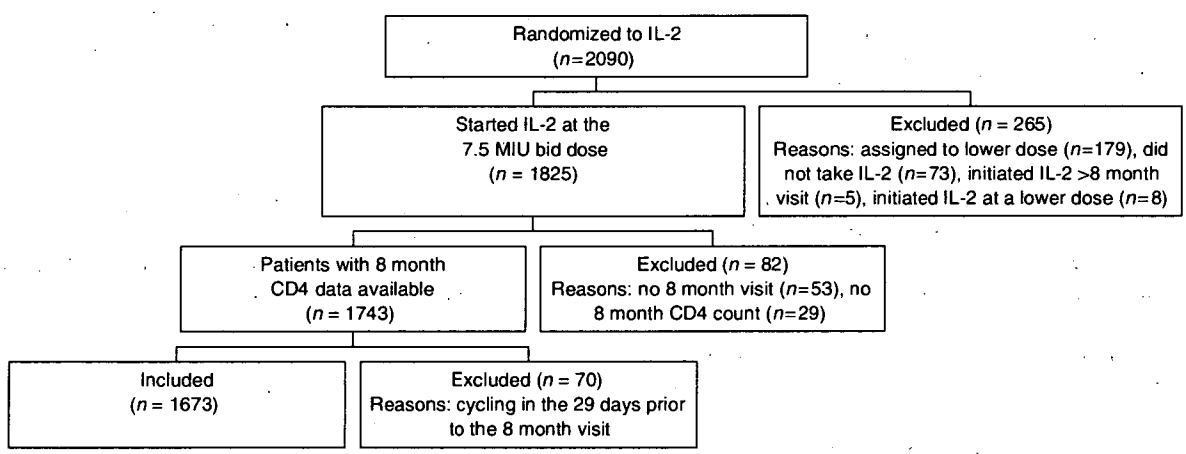

Fig. 1 Overview of patients receiving recombinant interleukin-2 (rIL-2) to 8 months of follow up.

Table 1 Baseline characteristics

Baseline parameter	All patients ($n = 1673$)
Age (years) [mean (SD)]	41.4 (8.8)
Gender [*n* (%) male]	1370 (82)
CDC category C [*n* (%)]	438 (26)
HIV-1 RNA (log_{10} copies/mL)[a] [median (IQR)]	1.7 (1.7, 2.6)
HIV-1 RNA < 500 log_{10} copies/mL [*n* (%)][a]	1311 (79)
Mean HIV-1 RNA in the past year (log_{10} copies/mL) [median (IQR)][a]	1.9 (1.7, 2.6)
CD4 (cells/μL) [median (IQR)]	461 (370, 587)
Last CD4 cell count prior to entry (cells/μL) [median (IQR)][a]	447 (351, 573)
Mean CD4 in the past year (cells/μL) [median (IQR)][a]	434 (346, 569)
Mean slope of CD4 cell count over the past year [median (IQR)][a]	30.4 (−121.5, 199.3)
CD4 % [median (IQR)][a]	24.0 (18.7, 30.0)
CD4 nadir (cells/μL) [median (IQR)]	190 (84, 293)
Time from nadir [median (IQR)] (years)	3.0 (1.0, 5.0)
Years since HIV diagnosis [median (IQR)][a]	6.0 (3.0, 10.0)
Months since ART [median (IQR)]	50.6 (28.2, 77.6)
BMI [median (IQR)][a]	23.7 (21.8, 25.8)
Hepatitis B/C/B + C coinfected [*n* (%)][b]	87/215/13 (6/15/1)
Risk group [*n* (%)]	
Same sex	807 (48)
IDU	132 (8)
Opposite sex	483 (29)
Blood products	26 (2)
> 1 risk factor	145 (9)
Other/unknown	80 (5)
Race [*n* (%)]	
White	1270 (76)
Black	150 (9)
Asian	186 (11)
Other	67 (4)
Concomitant medication [*n* (%)]	
PCP prophylaxis	90 (5)
Toxoplasmosis prophylaxis	22 (1)
Fungal prophylaxis	24 (1)
Herpes prophylaxis	84 (5)
Oral hypoglycaemic agents	33 (2)
Lipid-lowering drugs	151 (9)
Blood pressure-lowering drugs	89 (5)

[a]These Variables include missing data.
[b]Not all patients had hepatitis information available.
ART, antiretroviral; BMI, body mass index; CDC, Centers for Disease Control and Prevention; IDU, injecting drug use; IQR, interquartile range; PCP, pneumocystis pneumonia; SD, standard deviation.

IL-2 after the 8-month visit, and the remainder of patients did not have a CD4 cell count or had one within 29 days of their last cycle (Fig. 1).

The baseline characteristics of the 1673 patients included in these analyses are shown in Table 1. Patients were not at an advanced stage of HIV infection at baseline but many were highly treatment experienced. They were all ART experienced at baseline, predominantly male (82%), white (76%) and men who have sex with men (48%). The median [interquartile range (IQR)] CD4 cell count at baseline was 461 (370, 587) cells/μL, the nadir CD4 cell count was 190 (84, 293) cells/μL and the mean CD4 cell count in the year preceding baseline was 434 (346, 569) cells/μL. The median (IQR) baseline HIV-RNA value was 1.7 (1.7, 2.6) log_{10} copies/mL and 1311 patients (79%) had HIV-RNA < 500 copies/mL.

Patients had been on antiretroviral treatment a median (IQR) duration of 50.6 (28.2, 77.6) months and were exposed to a median (IQR) number of 5 (3,-7) ARTs. There were 687 patients (41%) who were using protease inhibitors (PIs) at baseline; 621 (37%) using nonnucleoside reverse transcriptase inhibitors (NNRTIs); 147 (9%) on both; and 218 (13%) on a nucleoside reverse transcriptase inhibitor (NRTI)-containing regimen only. The most common concomitant medications used at baseline were pneumocystis pneumonia (PCP) prophylaxis (5%) and lipid-lowering drugs (9%).

Immunological patterns prior to entry were evaluated for all individuals with three pre-baseline observations. Of the 1095 individuals with information, there was an increase in CD4 cell count for 611 patients (55.8%) in the year before entry. Overall, the median (IQR) yearly change in CD4 cell count in the absence of rIL-2 treatment, based on the CD4 cell counts in the year preceding baseline, was 30 (−122, 199) cells/μL.

Adherence to rIL-2

The median (IQR) dose of rIL-2 received was 75.0 (i.e. the full dose) (75.0, 75.0), 75.0 (60.0, 75.0) and 75.0 (60.0, 75.0) MIU over the first, second and third cycles, respectively. There were a total of 1375 patients (82%) who had completed at least three cycles by month 8. Patients who only completed one or two cycles received less rIL-2 during each corresponding cycle than patients who continued cycling ($P < 0.0001$ in both cases). Patients who only completed one cycle received a median (IQR) dose of 67.5 (45.0, 75.0) MIU during the first cycle and those who completed two received 60.0 (45.0, 75.0) MIU during their second cycle.

There were 638 patients (38%) who missed at least one of their 10 rIL-2 injections over the first three cycles; 23% of patients initiating rIL-2 missed at least one injection in the first cycle, 19% of patients initiating a second cycle missed at least one injection in the second cycle and 17% of patients initiating a third cycle missed at least one injection in the third cycle. These 638 patients included the 267 patients (16%) who dose-reduced in at least one of their first three cycles; 9% of patients had a dose reduction during the first cycle, 7% of patients who initiated more than one cycle dose-reduced during the second cycle and 4% dose-reduced during the third.